

High-Pressure Routes in the Thermoelectricity or How One Can Improve a Performance of Thermoelectrics[†]

Sergey V. Ovsyannikov^{*,‡,§,||} and Vladimir V. Shchennikov[‡]

[‡]High Pressure Group, Institute of Metal Physics of Russian Academy of Sciences, Urals Division, 18 S. Kovalevskaya Str., GSP- 170, Yekaterinburg 620041, Russia, [§]The Institute for Solid State Physics, The University of Tokyo, 5-1-5 Kashiwanoha, Kashiwa 277-8581 Chiba, Japan, ^{||}Institut de Minéralogie et de Physique des Milieux Condensés, Université Pierre et Marie Curie Paris 6 – CNRS, 140 rue de Lourmel, 75015 Paris, France, and ^{||}Bayerisches Geoinstitut, Universität Bayreuth, Universitätsstrasse 30, D-95447, Bayreuth, Germany

Received July 5, 2009. Revised Manuscript Received November 2, 2009

High pressure has a strong impact on materials. In regards to thermoelectrics, pressure is able to significantly improve their thermoelectric (TE) performance (i.e., power factor and figure of merit), and for this reason, pressure is a powerful tool for energy conversion technologies. This paper reviews studies on thermoelectric properties of relevant materials (PbTe, PbSe, Bi₂Te₃, Sb₂Te₃, and others) under pressure. It is figured out that enhanced thermoelectric properties of lead telluride and bismuth telluride appear beyond a range of energy gaps proposed for a “conventional” thermoelectricity in narrow-gap semiconductors. An example given for SmTe hints that pressure effects on the thermoelectric performance may be tremendous. This review also attends studies on high-pressure thermoelectric properties in the presence of a nonzero magnetic field. Influence of magnetic-field-related effects, such as magnetoresistance, magnetothermopower (Nernst–Ettingshausen effects), and Maggi–Reggi–Leduc effect is analyzed on examples of PbTe, PbSe, and Te. Problems related to both in situ measurements of transport properties under pressure, and practical realization of high-pressure (magneto-)thermoelectric devices are discussed. In summary, this review reports the state-of-the-art of pressure influence on thermoelectric materials and shows alternative poorly explored routes in the thermoelectricity.

1. Introduction

A search for alternative sources of energy remains an important task. Thermoelectric (TE) materials have the following uses: (i) heat-electricity conversion (thermoelectric generators), (ii) thermoelectric cooling, and (iii) measurement of temperature. The first two applications crucially depend on an efficiency of an element, which may be mathematically determined by the power factor (α) and the dimensionless figure of merit (ZT):

$$\alpha = \frac{S^2}{\rho}, ZT = \frac{T \times S^2}{\rho \times (\lambda_e + \lambda_{ph})} \quad (1)$$

where S is the thermopower, ρ is the electrical resistivity, $\lambda = \lambda_e + \lambda_{ph}$ is the thermal conductivity consisting of contributions of, respectively, electrons/holes (λ_e) and phonons (λ_{ph}), and T is the temperature.

The “classical” set of promising TE materials covering a range of temperatures from ~ 100 to 1000 Ks includes Bi–Sb, Bi₂Te₃, Sb₂Te₃, PbTe, Si–Ge, and some others.¹ The main obstacle preventing their commercialization is low ZT

parameters. By estimations,^{1–3} a discovery of a TE material with $ZT > 4$ would drastically increase the attractiveness of the TE cooling, and would result in a revolution in, for example, the refrigerator market. A reason why this task remained unsolved for several decades is a strong interrelationship between S , ρ , and λ_e parameters which are bound to an electron band structure; so, optimizing one of them we lose in other. Furthermore, the electronic part of the thermal conductivity (λ_e) is related to the electrical conductivity (σ) according to the Weidemann–Franz law as follows:^{4,5}

$$\lambda_e = L \times T \times \sigma, \quad (2)$$

where L is the Lorentz number. For metals the Lorentz number is close to $L_0 = 2.44 \times 10^{-8} \text{ W}^2/\text{K}^2$.^{4,5} Whereas for semiconductors, it may depend on many factors, and therefore, L is a function of temperature and pressure. For instance, for a nondegenerate electron gas $L = 1.55 \times 10^{-8} \text{ W}^2/\text{K}^2$,^{4,5} that is, appreciably lower than L_0 . Usually, the Weidemann–Franz law for semiconductors is utilized for determination of L by comparison of λ and σ .⁶

A traditional way to reach a maximal ZT is an “optimization” under variation in the concentration of charge carriers. This method is based on the fact that S , ρ , and λ_e depend on a carrier concentration in different ways, so a tuning of it can change ZT (in fact, more than one order).

[†] Accepted as part of the 2010 “Materials Chemistry of Energy Conversion Special Issue”.

*Corresponding author. E-mail: sergey.ovsyannikov@uni-bayreuth.de, sergey2503@gmail.com.

Such a circumstance hints that a search for an “influence parameter” that could “separate” S , ρ , and λ_e is probably a way to success. Measurements of S , ρ , and λ_e under alteration in T are also optimization-directed. Recent advances in improvement of ZT concerned ways of worsening of the thermal conductivity (eq 1), for example, in systems with (i) heavy elements (high atomic masses reduce the atomic vibration frequencies and hence λ_{ph}),³ and (ii) “introduced nanosize objects” which reduce λ but do not noticeably influence both S and ρ .⁷ In summary, a solution of the “thermoelectric problem” is being looked for in a technological plane, with a usage of doping,^{8,9} chemical substitution,^{10–18} variation in an interior geometry of TE element (nanostructures, superlattices, quantum dots, and wires),^{19–25} and variation in synthesis conditions.^{26,27} Some of recent intriguing achievements on the traditional TE telluride systems (Bi_2Te_3 , PbTe) are as follows: in Bi_2Te_3 – Sb_2Te_3 nanostructures, $ZT \sim 1.2$ – 1.47 at 300 K ^{28–31} and superlattices, $ZT = 2.4$ at 300 K ;³² in $\text{PbSeTe}/\text{PbTe}$ superlattices, $ZT = 1.6$ at 300 K ³³ and $ZT = 3$ at 550 K ;³⁴ in $\text{AgPb}_m\text{SbTe}_{2+m}$ ($m = 10, 18$) $ZT = 1.5$ – 2.2 at 700 – 800 K ;^{11,35–37} $ZT = 1.3$ – 1.7 at 650 K in nanostructured $\text{Na}_{1-x}\text{Pb}_{20}\text{Sb}_y\text{Te}_{22}$;³⁸ and in $\text{PbTe}:\text{Ti}$ $ZT = 1.5$ at 773 K .³⁹ Motivated by theoretical grounds, a search for new high-performance TE materials also resulted in some discoveries. Modern thermoelectrics are already not limited to “telluride” systems (besides those above-mentioned, there are other promising representatives, for example, Ag_9TlTe_5 ,⁴⁰ HfTe_5 ,⁴¹ ZrTe_5 ,⁴² thallium-rich tellurides,^{43,44} etc.), but they are related to completely different families. Some of them are Na_xCoO_2 ,^{45–49} filled skutterudites ($(\text{Ce},\text{La})\text{Fe}_{4-x}\text{Co}_x\text{Sb}_{12}$, $0 \leq x \leq 4$),² clathrates with a general formula $A_8B_{16}C_{30}$ (A) Eu, Ba, Sr, (B) Ga, Al, (C) Ge, Si, Sn),^{50–54} half-Heusler alloys (e.g., $(\text{Ti},\text{Zr},\text{Hf})\text{NiSn}$,⁵⁵ $(\text{Hf},\text{Zr},\text{Ti})\text{NiSn}$,⁸ $(\text{Zr},\text{Hf})\text{Co}(\text{Sb},\text{Sn})$,⁵⁶ etc.), Zintl compounds (e.g., Zn_4Sb_3 ,^{57,58} $\text{Yb}_{14}\text{MnSb}_{11}$,⁵⁹ bulk and low-dimensional transition metal oxides (e.g., SrTiO_3),^{60,61} and many others. High thermoelectric properties can manifest even in materials which were never considered as potential thermoelectrics. The brightest example of this is silicon, nanowires of which exhibit $ZT \sim 0.6$ – 1 at 200 – 300 K .^{62,63}

Since thermoelectrics should simultaneously possess both high thermoelectric and electrical properties (eq 1), one can surmise that some compromise ratio between them may be reached in a semiconducting material.⁶⁴ Figure 1 schematically shows a behavior of the thermopower, the electrical resistivity, and the thermal conductivity on the energy gap. One can find that the maxima of the thermoelectric power factor (efficiency) and the figure of merit (eq 1) are achieved at certain magnitudes of a forbidden gap. Notice, that in a general case the maxima locations of α and ZT do not coincide (Figure 1). In several studies, the optimal band gaps were calculated for two abstract systems, such as a “direct-gap” semiconductor (a prototype for PbTe)⁶⁵ and an “indirect-gap” semiconductor (a prototype for Bi_2Te_3).^{66,67} For indirect-gap semiconductors, the optimal band gap was found as $6k_B T$ ⁶⁶ or $10k_B T$,⁶⁷ where k_B is the Boltzmann’s constant

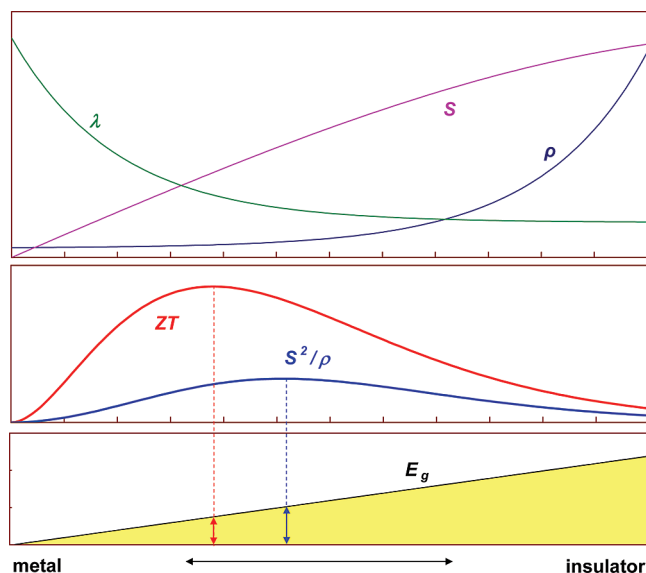


Figure 1. Schematic dependencies of the thermopower (S), the electrical resistivity (ρ), the thermal conductivity (λ), and the calculated by eq 1 thermoelectric power factor ($\alpha = S^2/\rho$) and figure of merit (ZT) on an energy gap.

and T is the temperature; for ambient T this gives $E_g \sim 0.15$ – 0.25 eV .^{66,67} For direct-gap semiconductors the optimal gap was found to be higher than $6k_B T$.⁶⁵ It was also claimed that the nonparabolicity of conduction and valence bands together with an ionized impurity scattering mechanism of carriers could significantly increase the optimal E_g in a direct-gap semiconductor and enhance ZT .⁶⁵

However, there are also examples of “unconventional” thermoelectricity, for example, InN ^{68–71} with a controversial $E_g \sim 0.6$ – 1 eV ⁷² and wide-gap $\text{In}_x\text{Ga}_{1-x}\text{N}$ solid solutions,⁷³ $\text{Cu}_2\text{ZnSn}_{1-x}\text{In}_x\text{Se}_4$ alloys with $E_g = 1.44\text{ eV}$,^{74,75} silicon nanowires.^{62,63} Thus, while an energy gap is a very important parameter of thermoelectrics, but either the interval of 6 – $10k_B T$ ^{65–67} is not universal and therefore does not cover all states promising for TE applications, or other parameters of electron band structure can overplay a band gap influence. Further, in a section reviewing the data of high-pressure effects on a thermoelectric performance, it is shown that even “conventional” thermoelectrics deviate from the “ 6 – $10k_B T$ law”.^{65–67}

There are some physical impacts which can significantly influence on a performance of thermoelectrics, for example, external pressure and magnetic field. Meanwhile, their effects on the thermoelectric parameters α and ZT are rarely investigated. Application of high pressure varies the density of materials and thus changes the intensity configuration of different electronic and magnetic interactions, resulting in different states. For instance, besides the conventional phonon mediated superconductivity, an unconventional magnetically mediated one has been revealed in “heavy fermion systems” under pressure;⁷⁶ further pressurization was reported to be able to reveal even more exotic forms of it.⁷⁷ Fragile metalloorganic crystals which were supposed not to be stable under pressure, in fact exhibit some chemical reactions or transitions to new dense forms.^{78–80} Uniaxial

pressure components can modify electron band structure, e.g., it was predicted that a tension along $\langle 111 \rangle$ in germanium is able to transmute it from indirect into a direct-gap semiconductor.⁸¹ An enormous potential of high pressure is also seen from the fact that its application to oxygen leads to a metal state which becomes superconducting below $T_c \sim 0.6$ K at ~ 100 GigaPascals (GPa).⁸² Another remarkable outcome of a high-pressure application is a transformation of elemental metallic sodium (Na) above 200 GPa to a transparent insulator with an energy gap of ~ 5 eV.⁸³

Like temperature, pressure also strongly influences on an electron band structure and in particular on an energy gap of a material. For this reason, an applied variable pressure is a very effective tool for thermoelectric technologies. Since conventional thermoelectrics are narrow-gap semiconductors with a tendency to metallization at relatively low pressures (e.g., ~ 5 – 7 GPa in Bi_2Te_3 ⁸⁴ and ~ 13 – 16 GPa in PbTe and PbSe),⁸⁵ a variation in such a narrow pressure interval permits modulation of E_g and hence searching for optimized TE states. An effect of pressure on the TE parameters may be “technical”, that is, variations in S and ZT arise owing to a disproportion in high-pressure alterations in S , ρ , and λ without qualitative changes in physical characteristics of a material. A more interesting case when pressure permits achievement of new electronic or structural states with the enhanced properties. These relatively low pressures may be in situ generated in plenty of various high-pressure chambers. Alternatively, they may be simulated in thin stressed films in which a film and a substrate have “misfit” lattice parameters that leads to stresses,^{86,87} or in high-pressure–high-temperature synthesis (HP–HT) which can either trap a high-pressure polymorph or partially keep high-pressure properties.^{26,88} The main reason why a promising method like pressure application is restrictedly used for TE goals is a lack of universal techniques which could permit simultaneous in situ measurements of all the three parameters needed (S , ρ , and λ) on a microsample under variation in pressure. Nowadays, simultaneous high-pressure electrical and thermoelectric measurements on the same sample are available,⁸⁴ but integrating them with the thermal conductivity remains challenging. One can combine electrical and thermoelectric data obtained in one experiment with those of thermal conductivity obtained in a different experiment. But in such a case, the ZT values that are achieved in a material may be only approximately estimated, as a modification in an electronic band structure is influenced by both all-round and uniaxial pressures, and it is difficult to reach exactly the same conditions in different transport techniques. The existing methods for measurement of thermal conductivity variation under pressure and temperature changes were applied basically for insulators and geological objects.^{89–96} Hopefully, the introduction of nanotechnologies to high-pressure field will assist in resolving these technical problems in the near future.

Magnetic field influences on thermoelectric, electrical and thermal properties in a different way and hence it is

also a powerful tool for TE technologies. Changes in the thermopower, the electrical resistivity, and the thermal conductivity in magnetic field are known respectively as Nernst–Ettingshausen effects, magnetoresistance, and the effect of Maggi–Reghi–Leduc.^{4,5} So, in a weak magnetic field,⁴ the values in eq 1 are transformed as follows:

$$S \rightarrow (S_0 + \Delta S_{\parallel} + \Delta S_{\perp}), \rho \rightarrow \rho(1 + \text{MR}),$$

$$\text{and } \lambda \rightarrow \lambda_0 + \lambda(B), \quad (3)$$

where S_0 is the thermopower in the absence of magnetic field ($B=0$), ΔS_{\parallel} and ΔS_{\perp} are, respectively, the contributions of the longitudinal and the transverse Nernst–Ettingshausen effects, and MR is the magnetoresistance. The magnetoresistance and Maggi–Reghi–Leduc effects are usually relatively small (about several percents), while a variation in the thermopower may be appreciable, basically owing to the presence of the transverse Nernst–Ettingshausen effect. Furthermore, this transverse effect is very sensitive to a sample’s geometry,⁹⁷ that gives one more possibility for optimization of the TE parameters. Positive effect of magnetic field on the TE performances of some materials was found in several works.^{97–103}

The above physical methods permit alternative viewing the central task of the energy conversion technologies. They suggest that taking promising thermoelectrics as a basis, one can perform a “multidimensional optimization” search under variation in doping, mesostructure, pressure, magnetic field, and in other parameters, and eventually one can achieve much higher thermoelectric performance than the starting one.

2. High-Pressure Effects on Thermoelectric Properties of Materials

To the moment an effect of applied pressure on the TE performance was investigated in a few materials. Among them a special attention was paid to classical telluride thermoelectrics based on Bi_2Te_3 and PbTe which are of the most interest because the maxima of their TE parameters are achieved around room temperature. These two systems were also intensively investigated by other high-pressure techniques, and so they are the most studied to the date. We will review works devoted to these two systems as well as some others. There is a set of different techniques for measurement of the thermopower under high pressure.¹⁰⁴ An interested reader can learn experimental details in cited papers.

2.1. Bismuth Telluride (Bi_2Te_3). Bismuth telluride (Bi_2Te_3) is one of the oldest among the basic materials for high-performance thermoelectric elements.^{64,105,106} Both n - and p -type Bi_2Te_3 -based TE solid solutions present a strong technological interest.^{28,31,32} At ambient conditions Bi_2Te_3 adopts a rhombohedral lattice of the $R\bar{3}m$ space group; the cell parameters in terms of hexagonal axes are as follows: $a_H = 4.383$ Å and $c_H = 30.487$ Å.^{107–110} A scenario of room-temperature pressure-driven phase transitions in Bi_2Te_3 remains obscure until the present. Originally, two

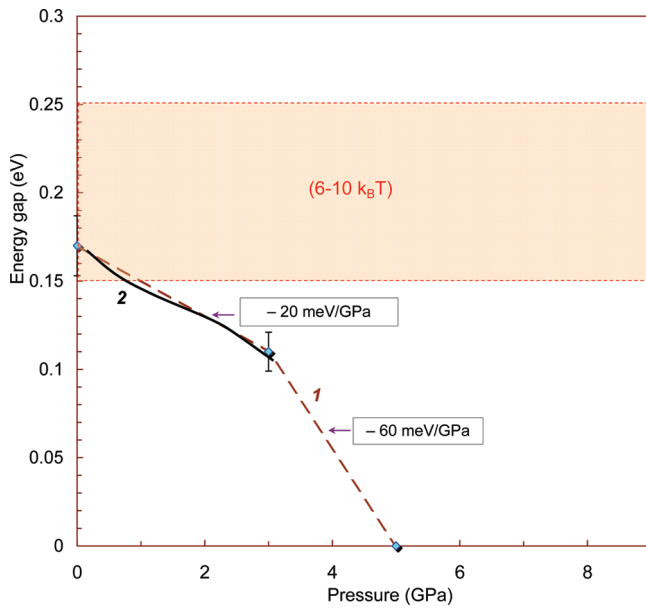


Figure 2. Qualitative pressure dependence of the energy gap in Bi_2Te_3 at ambient temperature. A proposed interval of optimized for the thermoelectricity energy gaps ($6-10 k_B T$) is shown.⁶⁵⁻⁶⁷ **1** the generalized data from ref 117, **2** the experimental data from ref 116. Usually, metallization is reached near 5–8 GPa.^{84,107-114}

transitions were found, first at ~ 6.7 GPa to another semiconductor phase and then at ~ 8.3 GPa to a metal.¹⁰⁹ The former remains an issue, whereas the latter has been confirmed in several studies.^{84,111-114} A very recent work claimed one more transition near 14 GPa,¹¹⁴ this correlates with found earlier jumps in the electrical resistivity near 15–17 GPa.¹¹⁵ A similarity in the pressure-driven phase transitions of Bi_2Te_3 and Sb_2Te_3 was recently shown.¹¹³ An indirect forbidden energy gap of Bi_2Te_3 is equal to $E_g \approx 0.17$ eV.^{110,116,117} It was established to decrease with pressure with a coefficient $dE_g/dP \approx -20$ (-60) meV/GPa before (after) 3 GPa. Hence, the gap closes near 5 GPa (Figure 2).^{110,117} It should be mentioned that the electron band structure of this material was investigated for several decades,¹¹⁸⁻¹²⁴ and to date, it still remains not properly understood.^{125,126} Thus, for example, it was recently found that an appropriate hole doping can significantly tune topology of Fermi surface toward to a 3D topological insulator.¹²⁶

“The-state-of-the-art” values of the figure of merit in $(\text{Bi,Sb})_2\text{Te}_3$ -based bulk thermoelectrics are somewhat above $ZT = 1$, and in some cases can reach 1.4.¹²⁷ This suggests that Bi_2Te_3 is a good candidate promising for achievement of tremendous values of the figure of merit (as high as 3 or 4) under different influences, such as applied pressure and magnetic field etc. Meanwhile, effects of pressure and magnetic field on TE properties of Bi_2Te_3 were investigated in only a few works.^{84,111,112,128,129}

Figure 3 summarizes some literature data on pressure behavior of the thermopower and the electrical resistivity in Bi_2Te_3 -based materials.^{84,111,112,128,130,131} Power factors, calculated in eq 1, are shown in Figure 4. It is apparently seen that pressure does a remarkable impact on the TE parameters of this family of thermoelectrics. Meanwhile, because of lacking data on pressure behavior

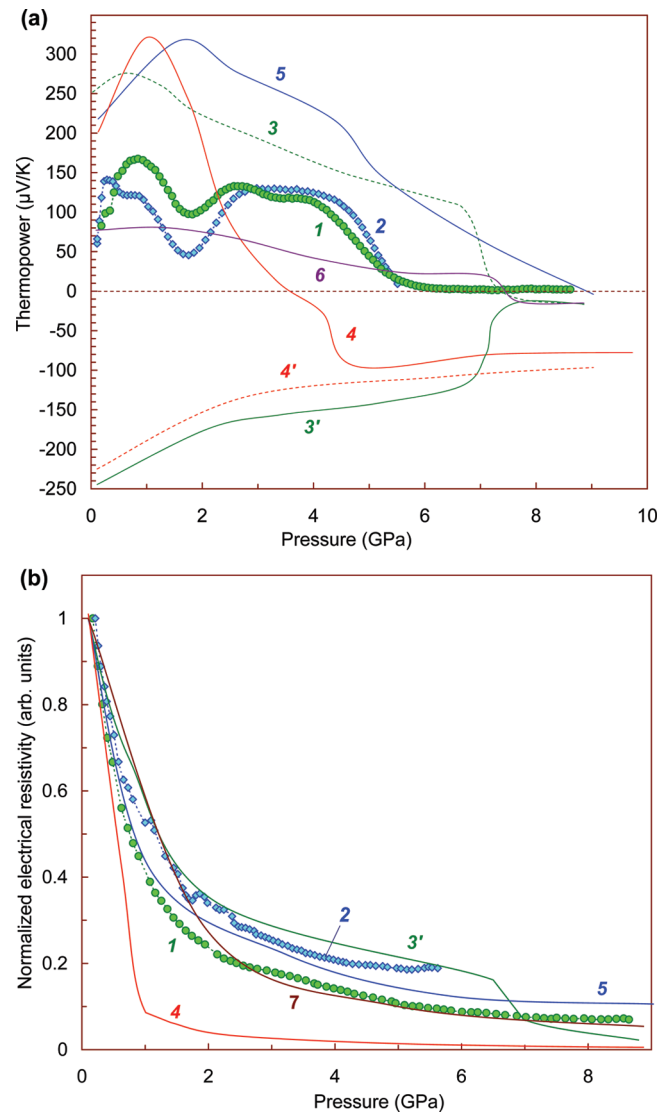


Figure 3. Pressure dependencies of the thermoelectric power (a) and the electrical resistivity (b) of Bi_2Te_3 -based materials at ambient T . **1** Bi_2Te_3 ($p = 3 \times 10^{18} \text{ cm}^{-3}$ at 4.2 K),⁸⁴ **2** $\text{In}_x\text{Bi}_{2-x}\text{Te}_3$ ($x = 0.04$) ($p = 3 \times 10^{17} \text{ cm}^{-3}$ at 4.2 K),⁸⁴ **3** and **3'** Bi_2Te_3 ($p = 1.2 \times 10^{19} \text{ cm}^{-3}$, $n = 1.1 \times 10^{19} \text{ cm}^{-3}$),¹¹¹ **4** and **4'** BaBiTe_3 ,¹²⁸ **5** $\text{Sb}_{1.5}\text{Bi}_{0.5}\text{Te}_3$,¹¹² **6** Sb_2Te_3 ($p \sim 8 \times 10^{19} \text{ cm}^{-3}$),¹³⁰ **7** Bi_2Te_3 .¹³¹

of the thermal conductivity, it remains unclear how much one can enhance ZT this way. There are possibilities for rough estimation of the thermal conductivity change with pressure. Thus, a variation in the lattice contribution (λ_{ph}) may be found with assistance of a model offered by Manga and Jeanloz.¹³² For elevated temperatures λ_{ph} comes as follows:¹³²

$$\lambda_{\text{ph}} \sim (\alpha/T)(1 + \varphi P/B_0) \quad (4)$$

where α is the thermal expansion coefficient, B_0 is the bulk modulus, and φ is the experimental factor (usually close to 7).¹³² The electronic part of the thermal conductivity (λ_e) may be estimated from the Weidemann–Franz law (eq 2) as it was mentioned in the introduction. Since, a pressure effect on L is unknown, it seems obscure how close one can approximate to the truth. For instance, the calculations for $\text{Sb}_{1.5}\text{Bi}_{0.5}\text{Te}_3$ performed in a typical

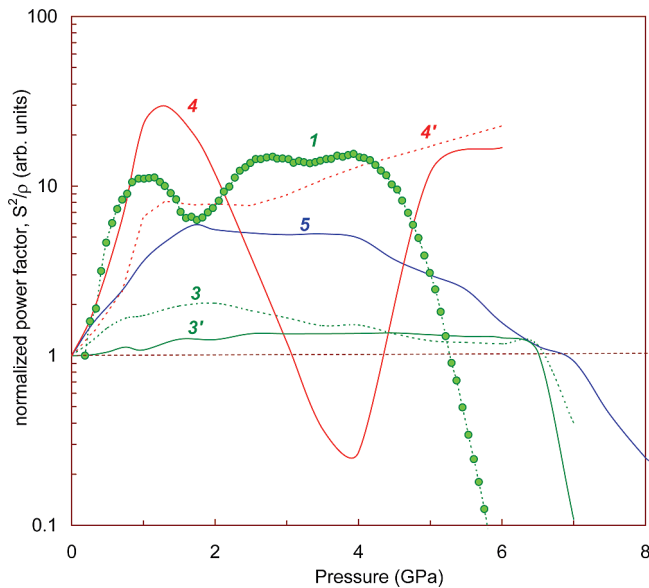


Figure 4. Pressure dependencies of the normalized power factor of the Bi_2Te_3 -based thermoelectrics calculated by eq 1 by the data from Figure 3. The numbers of the curves are the same as at Figure 3.

semiconductor approximation ($L = 1.55 \times 10^{-8} \text{ W}^2/\text{K}^2$)¹¹² strongly suggest only moderate increase in λ , and hence a possibility of multifold improvement in ZT. Thus, they found $\text{ZT} = 2.2$ at 1.7 GPa (Figure 4).¹¹² The only available experimental data on $\lambda(P)$ for Sb_2Te_3 shows very weak pressure effect on the thermal conductivity (a rise by $\sim 13\%$ to 1.6 GPa).¹³³

One can discern a qualitative difference in pressure dependencies of the thermopower of p - and n -type materials (Figure 3). Thus, the materials of p -type exhibit one or two maxima, which are absent in those of n -type (Figure 3). This leads to a higher pressure impact in the former (Figure 4). It is interesting to note that the enhanced TE properties are kept in Bi_2Te_3 -based materials (Figure 4) below the threshold of $6 k_B T$ (Figure 2). At the moment there is no generally recognized explanation of the maxima in the thermopower of p -type Bi_2Te_3 , $\text{Sb}_{1.5}\text{Bi}_{0.5}\text{Te}_3$, Sb_2Te_3 , and BaBiTe_3 (Figure 3). Likewise, there is no complete understanding how pressure changes the band structure of $(\text{Bi,Sb})_2\text{Te}_3$.¹³⁴ Thus, a maximum of ZT in $\text{Sb}_{1.5}\text{Bi}_{0.5}\text{Te}_3$ near 1.7 GPa (Figure 4, curve 5) was addressed to one of electronic ‘Lifshitz transitions’ consisting in a drastic change of Fermi surface topology;^{112,135} these transitions were in fact found in Bi_2Te_3 at helium temperatures.¹³⁶ At room temperature the Fermi surface is supposed to be strongly smeared. Nevertheless, changes in topology of electronic bands can modify effective masses and density of electron states,^{125,126,135,136} and hence, can tune TE properties. Band structure calculations of Sb_2Te_3 showed that a hydrostatic pressure results in only minor effects on the TE parameters, whereas uniaxial stress could lead to a strong enhancement of TE properties.¹²⁴ On the contrary, an experimental hydrostatic-pressure study found a 2-fold enhancement of the power factor in Sb_2Te_3 .¹³⁰ In ref 84 a pressure effect on a band structure of Bi_2Te_3 was proposed to issue from a competition between the contributions of the basic hole and the electron bands under narrowing in the forbidden

gap E_g on the one hand, and a contribution of an additional hole band which is rising owing to widening in ΔE_v (ΔE_v is an energy gap between the basic and additional hole bands) on the other hand (eq 5). Thus, while E_g is decreasing with pressure (Figure 2),^{110,116,117} ΔE_v was found to extend with a rate $dE_v/dP \sim +30 \text{ meV/GPa}$.¹³⁷ This suggests their competition and a strong dependence of a pressure effect on a starting holes concentration. Thus, a formula for the thermopower for Bi_2Te_3 was proposed as follows:⁸⁴

$$\frac{S}{k/|e|} = \left\{ \sum_i \frac{(\sigma_{pi} - \sigma_{ni})}{\sigma} \times (r + 2) + \sum_i \frac{(\sigma_{pi} - \sigma_{ni})}{\sigma} \times \frac{E_g}{2kT} + \frac{3}{4} \times \ln \frac{m_p^*}{m_n^*} + \frac{\Delta E_v}{kT} \times \frac{\sigma_{p2}}{\sigma} \right\}, \quad (5)$$

where, $\sigma = \Sigma(\sigma_{ni} + \sigma_{pi})$ is the total conductivity, m_p^* (m_n^*) is the effective mass of holes (electrons), and r is the scattering parameter of carriers. The index “ r ” corresponds to the electron and the hole bands, and the index “ 2 ” corresponds to the additional holes band.

It was shown that the additional band begin filling up when a holes concentration is higher than $p \sim 5 \times 10^{18} \text{ cm}^{-3}$.¹¹⁷ Qualitatively, an effect of the holes concentration on the maxima of Bi_2Te_3 - Sb_2Te_3 thermoelectrics one can see through the curves 1, 2, 3, and 6 in Figure 3. Thus, the “pure” single crystals of Bi_2Te_3 ($p = 3 \times 10^{18} \text{ cm}^{-3}$) and $\text{In}_{0.04}\text{Bi}_{1.96}\text{Te}_3$ ($p = 3 \times 10^{17} \text{ cm}^{-3}$) distinctly show two maxima (Figure 3a, curves 1 and 2, Figure 4, curve 1).⁸⁴ In a heavily doped p - Bi_2Te_3 ($p \sim 1.2 \times 10^{19} \text{ cm}^{-3}$) only the first one is kept (Figure 3, curve 3).¹¹¹ At very heavy doping (Sb_2Te_3 , $p \sim 8 \times 10^{19} \text{ cm}^{-3}$) the first maximum disappears too (Figure 3, curve 6).¹³⁰ Pressure-induced changes in the effective masses in eq 5 and corresponding variations in filling of the hole bands and their topology may also contribute to a thermopower value. The above consideration hints that a simultaneous optimization of the TE performance of Bi_2Te_3 -based elements under variation in both the holes concentration and pressure will be more effective than independent “tuning” of these parameters.

The existence of some distorted rhombohedral phase (with a modified band structure) in Bi_2Te_3 which was proposed to appear before the metallization around 4–8 GPa (Figures 2 and 3)^{107–109} could explain the second hump in the thermopower (Figure 3). In very recent X-ray diffraction studies^{84,114} some anomalies in pressure dependencies of the lattice parameters of the rhombohedral lattice were in fact registered. However, at the moment there is not sufficient evidence to claim it. Earlier, it was predicted that contraction of this layered structure bound by weak van der Waals forces may have different regimes;¹³⁸ first, the c axis (perpendicular to the layers) rapidly shrinks, and when the interatomic distances inside the layers become close to the distance between neighboring layers, a compression regime is expected to be changed.¹³⁸ Moreover, a very recent thorough study on a

family $(\text{Bi,Sb})_2(\text{Te,Se})_3$ revealed a tendency to form natural nanostructures which modulate structural properties.¹³⁹ This suggests that a method of synthesis of a sample plays a significant role.¹³⁹ Thus, this problem of possible pressure-driven structural distortion in the rhombohedral lattice of Bi_2Te_3 remains unresolved.

It is worthy to mention pressure studies on other bismuth chalcogenides, namely Bi_2Se_3 and Bi_2S_3 . Thus, in several Bi_2Se_3 -based thermoelectrics a significant positive pressure effect on the TE performance was found (e.g., in $\beta\text{-K}_2\text{Bi}_8\text{Se}_{13}$).¹⁴⁰ Bulk Bi_2S_3 has much lower TE parameters than those in Bi_2Te_3 . However, recently it was demonstrated that in nanorods of Bi_2S_3 one can achieve very high values of the power factor,¹⁴¹ and hence this material may be also of interest for the thermoelectricity. So far, the only work that probed the TE properties of bulk Bi_2S_3 up to 2.5 GPa found no appreciable effects.¹⁴²

2.2. Lead Telluride (PbTe). Lead telluride (PbTe) is the second important thermoelectrics of which maximum of ZT lies around ambient temperatures (in fact, shifted to elevated ones while still appreciable high at ambient).¹⁴³ Both *n*- and *p*-type PbTe-based TE elements are utilized.¹⁴³ At ambient conditions, PbTe adopts a NaCl structure with a lattice parameter $a = 6.462 \text{ \AA}$.¹⁴⁴ The ambient semiconductor gap of PbTe is direct and equal to $E_g \approx 0.29 \text{ eV}$.¹⁴⁵ In many studies, it was established that pressure application leads to its narrowing with a coefficient $dE_g/dP \sim -(70-90) \text{ meV/GPa}$.¹⁴⁵ A kindred semiconductor, PbSe is also a promising thermoelectric, though it trails PbTe in TE performance.¹⁴³ It is characterized by $E_g \approx 0.26 \text{ eV}$ and $dE_g/dP \sim -(60-86) \text{ meV/GPa}$.¹⁴⁵⁻¹⁴⁷ A gapless state was found in the both compounds near 3 GPa.⁸⁵ The pressure behavior of E_g in PbTe and PbSe constructed by the literature data is compared at Figure 5. Under pressure NaCl phases normally transform to denser metallic CsCl ones. In PbTe one intermediate phase was found to be stable between $\sim 6-7$ and $\sim 13 \text{ GPa}$.¹⁴⁸⁻¹⁵⁰ Only recently has this phase been reliably refined in the orthorhombic symmetry (*Pnma* space group, no. 62).^{151,152} A behavior of PbSe is more complicated as it may have more than one phase in an intermediate region from 4–5 up to 15–16 GPa.¹⁵³ The intermediate phases in both PbTe and PbSe were experimentally found to be indirect gap semiconductors⁸⁵ with $E_g \sim 0.1 \text{ eV}$ and $\sim 0.4 \text{ eV}$, respectively.¹⁵⁴ After the refinement of the orthorhombic phase of PbTe in the *Pnma* symmetry,^{151,152} the band structure calculations reproduced the indirect character of its gap and found $E_g = 0.166 \text{ eV}$ at 6.5 GPa;¹⁵⁵ notice that for *Pnma*-PbSe, recent calculations found an indirect gap of $E_g = 0.27 \text{ eV}$ at 9.5 GPa.¹⁵⁶

“The-state-of-the-art” ambient ZT values of PbTe and PbSe bulk crystals are normally around ~ 0.4 and ~ 0.3 , respectively,¹⁴³ i.e., lower than the one in Bi_2Te_3 .¹²⁷ While, because of a stronger pressure-driven narrowing in E_g (Figure 2 and Figure 5), a pressure impact on the TE performance may be higher. Investigations of pressure effect on transport properties of PbTe were started several decades ago but they were limited to $\sim 1 \text{ GPa}$.^{157,158} To the moment in situ measurements of the TE properties of PbTe under

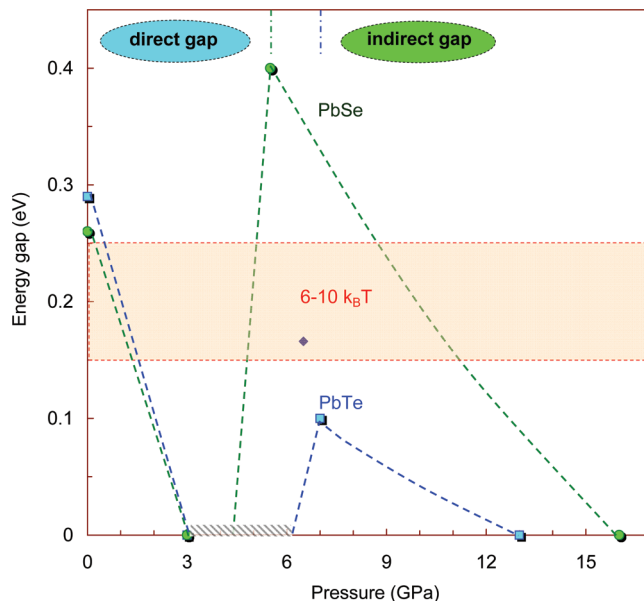


Figure 5. Qualitative pressure dependencies of the energy gap in PbTe and PbSe at ambient temperature. A proposed interval of optimized for the thermoelectricity energy gaps ($6-10 k_B T$) is shown.⁶⁵⁻⁶⁷ The ambient E_g values and their pressure coefficients ($dE_g/dP \approx -(60-86)$ and $-(70-90) \text{ meV/GPa}$ respectively for PbSe and PbTe) were taken from ref 145. A gapless state in both PbTe and PbSe was found near 3 GPa.⁸⁵ The E_g values at the high-pressure phases were taken, respectively, for PbSe and PbTe to be ~ 0.4 and $\sim 0.1 \text{ eV}$.¹⁵⁴ Band structure calculations for *Pnma*-PbTe at 6.5 GPa found $E_g \sim 0.166 \text{ eV}$.¹⁵⁵ Finally, above $\sim 13-16 \text{ GPa}$ PbTe and PbSe transform to a metal CsCl-structured phases.⁸⁵

high pressure were carried out in only a few works.^{154,159-162} A series of works was devoted to HP-HT synthesis of PbTe-based thermoelectrics.^{26,88,163} Notice, that nowadays PbTe and PbSe may be grown in different shapes (e.g., nanoboxes, dendrites flower-like nanocrystals, etc),¹⁶⁴⁻¹⁶⁹ and therefore there are more possibilities for their applications.

It was expected that both the electrical resistivity and the thermopower will dramatically diminish with pressure owing to a closing of the energy gap, and a possible improvement of the power factor could result from the difference in the decrease rates. In fact, it has been established that HP-HT synthesis (which partly keeps high-pressure properties) results in a considerable drop in the electrical resistivity under a moderate decrease in the thermopower;^{26,88} as a sequence a significant enhancement of α and ZT is achieved.^{26,88} However, in situ measurements on single crystals revealed a more complicated behavior (Figure 6).^{154,159-161} Thus, in *p*-type PbTe samples an inversion of the thermopower was found at the initial NaCl-structured phase (Figure 6). This results in a nonmonotonic dependence of the power factor on pressure (Figure 7). A new promising for the thermoelectricity state is revealed near 1.5–3 GPa: the thermopower value is as high as the ambient one but has the opposite sign, and the electrical resistivity is one or two orders lower (Figures 6,7).¹⁶¹ A magnitude of this falling of the resistivity likely depends on a starting value. It is worthy to mention one work which found a small jump in the resistivity of $\text{Pb}_{0.92}\text{Ge}_{0.08}\text{Te:Ga}$ near 2 GPa,¹⁷⁰ in agreement with the thermopower enhancement around this pressure value (Figure 6).

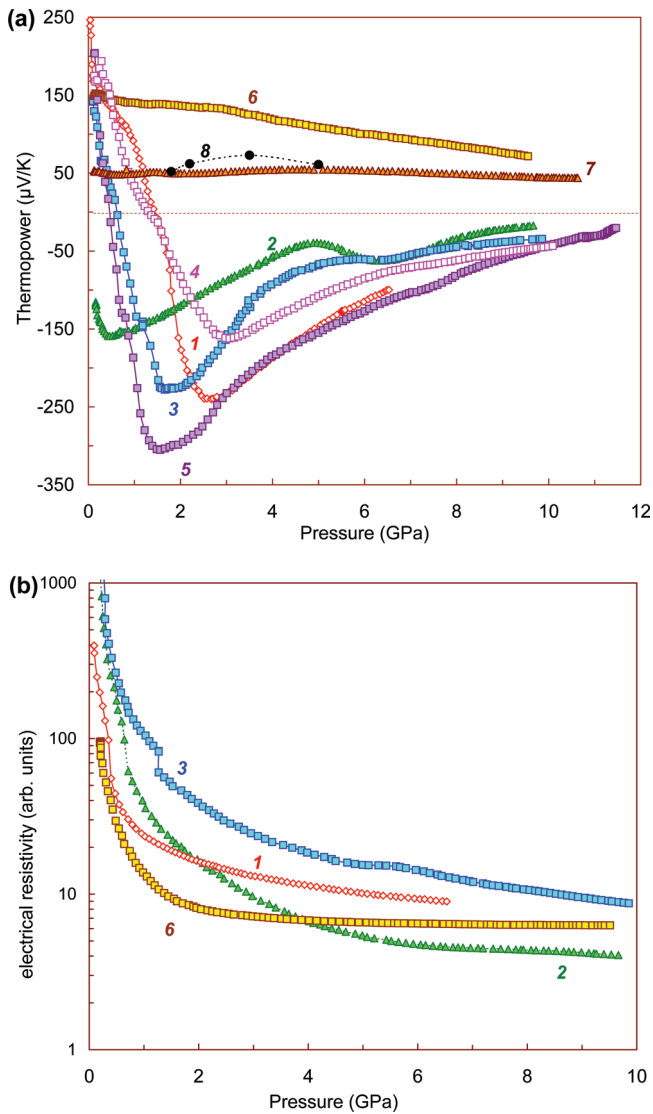


Figure 6. Pressure dependencies of the thermopower (a) and the electrical resistivity (b) of PbTe-based materials at ambient T . 1 p -PbTe doped with Si $\sim 5 \times 10^{-3}$ at%,¹⁶¹ 2 n -PbTe ($n = 1.5 \times 10^{18} \text{ cm}^{-3}$),¹⁶¹ 3 p -Pb_{0.55}Te_{0.45},¹⁶¹ 4 p -Pb_{0.45}Te_{0.55} doped with Si $\sim 10^{-3}$ at%,¹⁶⁰ 5 p -Pb_{0.95}Mn_{0.05}Te,¹⁶⁰ 6 p -Pb_{0.393}Sn_{0.157}Te_{0.45},¹⁶¹ 7 p -Pb_{0.71}Sn_{0.29}Te,¹⁶⁰ 8 PbTe at 350 K.¹⁶²

The colossal improvement of the power factor in PbTe is achieved beyond the proposed belt of optimized for the thermoelectricity energy gaps ($6\text{--}10 k_B T$) (Figure 5).^{65–67} The origin of this improvement could be related to not properly understood pressure effects on the edge of the valence band which includes the bands of light and heavy holes;⁵ the former is basic, while the latter normally lies below and does not contribute much to conductivity. It was found that a rise in temperature leads to the opposite shift effects for these two bands.⁵ The microhardness of PbTe-based materials of p -type was established to depend on the carrier concentration above $p \sim 5 \times 10^{18} \text{ cm}^{-3}$.¹⁷¹ This puzzling fact was explained by a contribution of this heavy holes band which begins to fill up when the concentration exceeds the above-mentioned.¹⁷¹

One more maximum in the power factor appears near 6.5 GPa (Figure 7). Apparently, this feature originates from the high-pressure $Pnma$ polymorph of PbTe.^{151,152} The pressure-driven transition from the NaCl to the

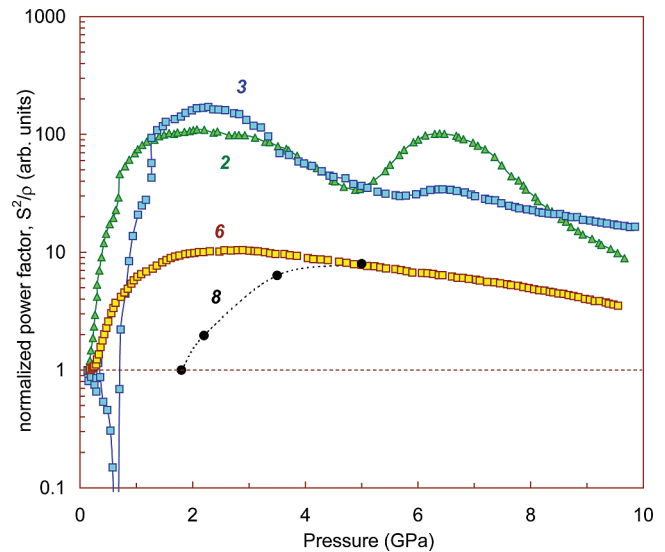


Figure 7. Pressure dependencies of the normalized power factor of some of the PbTe-based thermoelectrics calculated by eq 1 by the data from Figure 6. The numbers of the curves are the same as at Figure 3. Curve 8 was normalized by the power factor value at 1.8 GPa.¹⁶²

$Pnma$ structure is accompanied by an opening of the indirect energy gap (Figure 5),^{85,155} and hence both the thermopower and electrical resistivity are expected to exhibit jump-like anomalies on the transition. Experimentally, it has been established that a growth in the resistivity is much less than the one in the thermopower,¹⁵⁴ and therefore a win in the power factor is achieved (Figure 7). Band structure calculations also suggest that $Pnma$ -PbTe is an excellent thermoelectric with $ZT = 0.9$ (1.59) at 300 (600 K) at 6.5 GPa.¹⁵⁵

It is interesting to estimate the values of the figure of merit in PbTe which potentially may be achieved near 1.5–3 GPa (Figure 7). Since the starting values of the electrical resistivity of the PbTe single crystals were about several $\text{m}\Omega \times \text{cm}$,^{159–161} to 2–3 GPa they are expected to be equal to $\sim 0.1 \text{ m}\Omega \times \text{cm}$. The absolute thermopower values for these pressures are about 200–250 $\mu\text{V}/\text{K}$ (Figure 6). A pressure effect on the thermal conductivity may be roughly estimated by the Weidemann-Franz law (eq 2) and the above-discussed Manga–Jeanloz model (eq 4).¹³² The former permits rough estimation of λ_e as follows: $\lambda_e = L \times T \times \sigma \sim 1.55 \times 10^{-8} \text{ W}^2/\text{K}^2 \times 300 \text{ K} \times 10^6 (\Omega \times \text{m})^{-1} = 4.65 \text{ W}/(\text{K} \times \text{m})$. The latter suggests that $\lambda_{\text{ph}}(P = 3 \text{ GPa}) \sim \lambda_{\text{ph}}(P = 0) \times (1 + \varphi P/B_0)$. Taking B_0 as 39.8 GPa,^{144,145} ambient λ_{ph} as 1.7 $\text{W}/(\text{K} \times \text{m})$,^{144,145} and $\varphi = 7$,¹³² it comes as follows: $\lambda_{\text{ph}}(P = 3 \text{ GPa}) \approx 1.7 \text{ W}/(\text{K} \times \text{m}) \times (1 + 7 \times 3 \text{ GPa}/39.8 \text{ GPa}) \approx 2.6 \text{ W}/(\text{K} \times \text{m})$. Thus, $\lambda(P = 3 \text{ GPa}) = \lambda_e + \lambda_{\text{ph}} = 2.6 + 4.65 = 7.25 \text{ W}/(\text{K} \times \text{m})$; this suggests more than 4-fold rise in λ , whereas available experimental data up to 1.6 GPa evidence an increase in the total thermal conductivity only by ~ 40 and $\sim 70\%$ for two samples of PbTe.¹³³ Hence, $ZT = T \times S^2/(\rho \times \lambda) = 300 \text{ K} \times (200\text{--}250 \mu\text{V}/\text{K})^2/(0.1 (\text{m}\Omega \times \text{cm}) \times 7.25 \text{ W}/(\text{K} \times \text{m})) \sim 1.7$ and ~ 2.6 for $S = 200$ and $250 \mu\text{V}/\text{K}$, respectively. Normally, increase in temperature enhances the TE performance of PbTe-based compounds,¹⁶² so at elevated temperatures, higher $S^2/(\rho \times \lambda)$ values are expected.

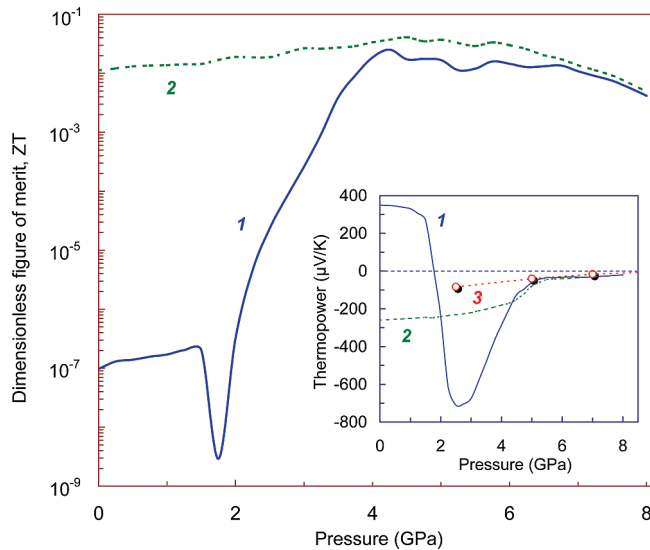


Figure 8. Pressure dependencies of the dimensionless figure of merit (ZT) of SmTe at ambient temperature calculated by data on pressure dependencies of the electrical resistivity, the thermopower, and the thermal conductivity from ref 177. The insert shows the examples of pressure dependencies of the thermopower. *1* stoichiometric, *2* doped with Sm,¹⁷⁷ and *3* for SmTe from ref 192.

Thus, pressure appears to be an effective tool to improve the TE performance of PbTe. One may propose similar pressure effects in other lead chalcogenides, namely, isostructural PbSe and PbS which are believed to have kindred electron band structures.¹⁴⁵ However, hitherto only very moderate positive pressure effects were experimentally established up to 0.5 GPa, whereas their high-pressure polymorphs were found to be poor thermoelectrics.¹⁶¹ Under further pressure increase, both PbSe and PbS reach optimized energy gaps near ~ 9 – 12 and 11 – 14 GPa, respectively (Figure 5).¹⁵³ Available literature data do not support a possibility of excellent TE properties near these pressures.¹⁵⁹ The case of PbSe which shows a resembling to PbTe $E_g(P)$ behavior at the NaCl phase (Figure 5) hints that the colossal improvement in PbTe under pressure near 1.5–3 GPa arises not only owing to the narrowing of E_g , but is related also to other modifications in the electron band structure (Figure 7). This circumstance evidence limitations of the approaches that directly bind TE properties and value of energy gap.^{65–67}

2.3. Other Compounds. From time to time promising new thermoelectrics for ambient temperatures are synthesized. Some of them have been already mentioned in the introduction. TE properties were examined under pressure in only a limited number of them, and a positive (and often significant) pressure effect on the TE performance was found, for example, in $\text{Nd}_x\text{Ce}_{3-x}\text{-Pt}_3\text{Sb}_4$,^{135,172} $\text{Bi}_2\text{Sr}_2\text{Co}_2\text{O}_9$,¹⁷³ tin clathrates ($\text{Cs}_8\text{Sn}_{44}$),¹⁷⁴ AgSbTe_2 ,²⁷ HgTe ,^{175,176} SmTe ,¹⁷⁷ SnSe ,¹⁷⁸ and in some others. Thus, for instance, undoped SmTe with a negligible ambient figure of merit $ZT \sim 10^{-7}$ demonstrates a remarkable improvement of its TE properties under compression to 4 GPa (Figure 8). Its ZT grows by a factor of $\sim 10^5$ and becomes comparable with those of poor thermoelectrics (Figure 8). This example apparently

shows how much pressure can be effective in energy conversion technologies.

3. Combined Effects of Pressure and Magnetic Field on Thermoelectric Properties

Magnetic field (B) can influence on all the parameters in eq 1 and for this reason it can change the TE performance. The effects of magnetic field on the electrical resistivity, the thermopower, and the thermal conductivity are known, respectively, as the magnetoresistance effect, the magnetothermopower (the Nernst–Ettingshausen effects), and the Maggi–Reggi–Leduc effect.^{4,5,179} The Nernst–Ettingshausen (N–E) effect consists of (i) a longitudinal contribution (variation in the thermopower along a temperature difference in a transverse magnetic field) and of (ii) a transverse one (an appearance of a thermoelectric voltage (U) in the direction perpendicular to both a thermal flow and a magnetic field (i.e., in the “Hall” direction)). In a simple case of an intrinsic semiconductor with one-band conductivity, the transverse magnetoresistance (MR), the longitudinal N–E effect ($\Delta S_{||}$), and the coefficient of the transverse N–E effect (Q) in weak magnetic fields ($\mu B < 1$) come as follows:^{4,179}

$$\text{MR} \equiv \frac{\Delta\rho(B)}{\rho} = A_1 \times (\mu \times B)^2, \quad (6)$$

$$\Delta S_{||}(B) = A_2 \times \left(\frac{k}{e}\right) \times (\mu \times B)^2, \quad (7)$$

$$Q = A_3 \times r \times \left(\frac{k}{e}\right) \times \mu, \quad (8)$$

where, e is the electron charge, k is the Boltzmann’s constant, $\mu = e \times \tau / m$ is the mobility of charge carriers, m is the effective mass, τ is the impulse relaxation time of charge carriers, and r is the scattering parameter describing a dependence of τ on the electron energy ε , $\tau(\varepsilon) \approx \varepsilon^r$.^{4,179} The constants A_1 , A_2 , and A_3 are the functions of r and are determined by Fermi integrals.^{4,179} A sign of Q is directly determined by a sign of the parameter r . $\Delta S_{||}$ depends on r in a hidden manner (eq 7) but also changes its sign if the one of the parameter r is changed; for example, for two opposite cases of scattering by (i) acoustic phonons ($r = -1/2$) and by (ii) charged centers ($r = 3/2$), the constant A_2 respectively equals to $A_2 \approx 9\pi/16(1-\pi/8)$ and $A_2 \approx -30$, and so a value of the thermopower either increases ($r = -1/2$) or decreases ($r = 3/2$) with B .^{4,179}

The main peculiarity of the N–E effects consists in their direct dependence on carrier mobility (eqs 7 and 8). Hence, conditions for optimization of thermoelectric and magnetothermoelectric effects essentially distinguish. For instance, the appearance of minority charge carriers of opposite sign is expected to diminish the thermopower value because of “annihilation” of electron and holes contributions.⁶⁵ Whereas magnetothermoelectric effects

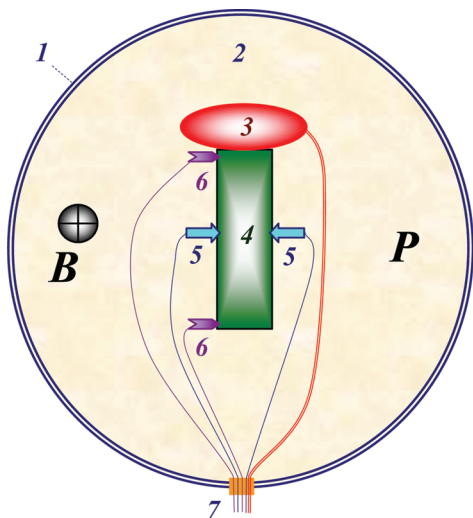


Figure 9. A standard scheme for measurement of the longitudinal and the transverse Nernst–Etingshausen effects under pressure P . A magnetic field B is directed perpendicularly to the plot's plane. 1 shows a high-pressure working volume; 2 A pressure-transmitting medium (fluid); 3 An electrical heater for production of a temperature difference along the longest size of a sample 4 ; 5 and 6 the probes and thermocouples for transverse $5-5$ and longitudinal $6-6$ measurements, 7 , the electrical wires.

on the contrary are enhanced in a case of two-band conductivity.^{85,180} Measurement of a set of electrical, thermoelectric, galvanomagnetic, and magnetothermoelectric properties in a sample permit determination of basic parameters of its electron band structure, such as concentration, mobility, effective mass, and scattering parameter of carriers. Thus, a so-called “four coefficient method” which extracts the above parameters from four properties (electrical conductivity, thermopower, Hall, and N–E effects),¹⁸¹ is actively applied nowadays.^{12,13,182} However, its full high-pressure realization is challenging.

Significant impacts of magnetic field on the TE performance were experimentally observed in some compounds.^{98–100,102} For instance, in $\text{Bi}_{0.91}\text{Sb}_{0.09}$ a magnetic field of 0.5 T improved ZT by a factor higher than 2, and so at 140–180 K ZT reached $\sim 1.2-1.3$.¹⁰⁰ A combined effect of magnetic field and pressure on the TE parameters could be more significant than those are achieved in separate studies. Because of experimental difficulties in parts of measurement of the Nernst–Etingshausen and Maggi–Reghi–Leduc effects, such investigations were carried out in only a few works.^{85,104,180,183–187} Figure 9 shows a classical scheme for measurement of the longitudinal and transverse N–E effects, which may be realized for bulk samples up to 2–3 GPa.¹⁸³ Another approach shown in Figure 10 makes it possible to measure the N–E effects at pressures as high as 30 GPa and beyond.⁸⁵ The latter approach (Figure 10) permits managing with only one pair of electrical probes, since the longitudinal N–E effect is measured from the thickness of a sample (Δy in Figure 10c) and a contribution of the transverse one may be measured from the “Hall projection” of the distance between the electrical probes (Δx in Figure 10c). In this approach, the electrical probes always output the longitudinal effect, while the transverse one

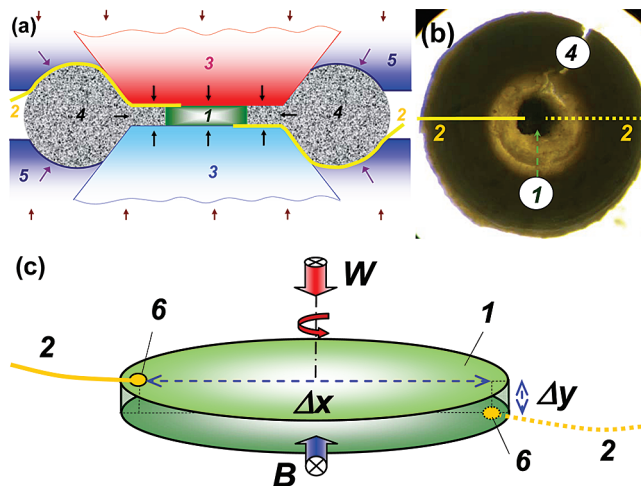


Figure 10. A scheme for measurements of the longitudinal and the transverse Nernst–Etingshausen (N–E) effects under pressure P in flat samples (after ref 104). 1 , a sample; 2 , the electrical probes; 3 , the anvil insets (made of sintered diamonds) in the high-pressure plungers; 4 , a container made of the lithographic stone; 5 , the supporting hard-alloy matrices (plungers); and 6 , the ends of the electrical probes. (a): A side view of a high-pressure cell. The arrows show acting forces. (b): A photograph of a container 4 of ~ 2 mm in diameter recovered from high pressure. The black circle in the center is a sample of ~ 300 μm in diameter and ~ 20 μm in the thickness. The electrical probes are shown schematically. (c): the block arrows W (perpendicular to the plane of a sample) and B (parallel to the one) show the directions of a thermal flow and magnetic field, respectively. The longitudinal N–E effect is output from the Δy distance, while the transverse N–E one from the Hall projection of the Δx distance. By turning a cell with a sample around its axis of symmetry (parallel to W) one can change the transverse N–E effect (eq 9).

may be modulated by a turning of a high-pressure cell with a sample around its axis in a nonzero magnetic field (Figure 10c). The N–E effects are simply separated as the longitudinal is quadratic (eq 7), whereas the transverse one is linear on B (eqs 8 and 9).^{4,179} Notice that the full transverse effect (ΔS_{\perp}) strongly depends on geometrical parameters as follows:¹⁰⁴

$$\begin{aligned} \frac{\Delta U_{\perp}(B)}{\Delta x} &= Q \times B \times \frac{\Delta T}{\Delta y} \Rightarrow \frac{\Delta U_{\perp}(B)}{\Delta T} \equiv \Delta S_{\perp} \\ &= Q \times B \times \frac{\Delta x}{\Delta y}. \end{aligned} \quad (9)$$

This means that by variation in the geometrical parameters ($\Delta x/\Delta y$ ratio) one can additionally enhance the magnetothermopower effects.⁹⁷

A direct measurement of Maggi–Reghi–Leduc effect (a variation in the thermal conductivity in magnetic field) under pressure remains a challenging task. For intrinsic nondegenerate electron gas in weak magnetic fields ($\mu B < 1$), a dependence of the electron part of the thermal conductivity comes as follows:¹⁸⁸

$$\lambda_{ie}(B) = n_i \mu_i \left(r + \frac{5}{2} \right) \frac{k^2 T}{e} \{ 1 - a_{r1} (\mu_i B)^2 \}, \quad (10)$$

where n_i is the i 's carrier concentration and a_{r1} is a multiplier depending on r . Notice, that for any scattering mechanism ($-1/2 \leq r \leq 3/2$), λ_e diminishes with B .

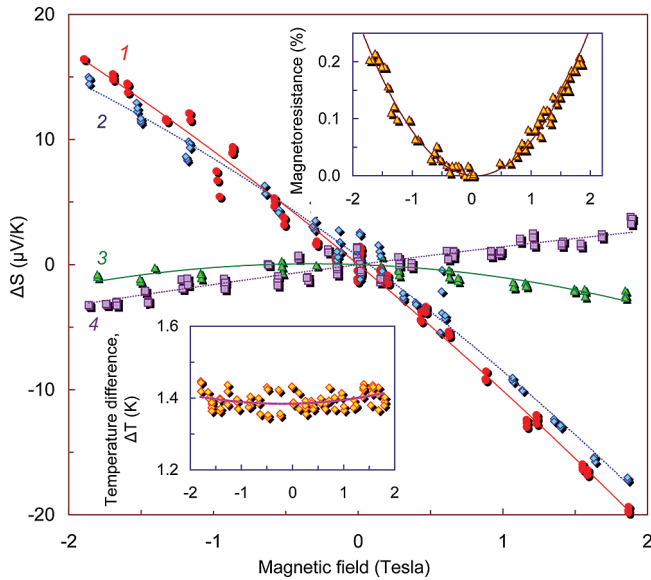


Figure 11. Variation in the thermopower of PbTe in magnetic field at pressure 2.6 GPa and ambient temperature.⁸⁵ The curves were obtained under turning of a high-pressure cell around its axis (see Figure 10c). Position 1 exactly corresponds to the case shown in Figure 10c, that is, the distance between the contacts Δx is perpendicular to the directions of magnetic field B and a thermal flow W . Thus, the curve 1 is a superposition of the maximal transverse and the longitudinal Nernst–Ettingshausen effects. The positions 2, 3, and 4 correspond to turning by, respectively, $\sim 10^\circ$, 90° , and 110° from the position 1. The curve 3 corresponds to the almost pure longitudinal N–E effect (eq 7). The insets show the magnetoresistance effect and a variation in a temperature difference (ΔT) in PbTe in magnetic field near 3 GPa from refs 85, 187.

In stationary thermal regime, a temperature difference along a sample thickness ΔT is equal to $\Delta T = q \times \Delta y / (\lambda_{\text{ph}} + \lambda_e)$, where q is the density of the thermal flux and Δy is the thickness of a sample. For a typical semiconductor case (i.e., $\lambda_{\text{ph}} \gg \lambda_e$) using eq 10 one can derive an expression as follows:¹⁸⁷

$$\begin{aligned} \Delta T &= q \times \Delta y / (\lambda_{\text{ph}} + \lambda_e(B)) \sim q \times \Delta y / \lambda_{\text{ph}} \\ &\quad \times [1 - \lambda_e(B) / \lambda_{\text{ph}}] \\ &= q \times \Delta y / \lambda_{\text{ph}} \\ &\quad \times \left[1 - n\mu / \lambda_{\text{ph}} \left(r + \frac{5}{2} \right) \frac{k^2 T}{e} \{1 - a_{r1}(\mu B)^2\} \right] \\ &= \Delta T(0) + \beta \times (\mu B)^2 \end{aligned} \quad (11)$$

where β is the coefficient depending on r , λ , n , μ , and T .

Figure 11 summarizes experimental data on magnetic field effect on the resistivity, the thermopower and a temperature difference along a sample (related to the thermal conductivity) of PbTe near 3 GPa.^{85,187} One can see that a magnitude of a variation in the thermopower exceeds the one in the resistivity (Figure 11). A very weak quadratic dependence of a temperature difference (inset in Figure 11) suggests that a corresponding change in the thermal conductivity is negligible. The variation in the thermopower changes its sign in dependence on the pole of magnetic field (Figure 11). Hence, both in n - and p -type samples one can enhance $|S|$. Hitherto the maximal

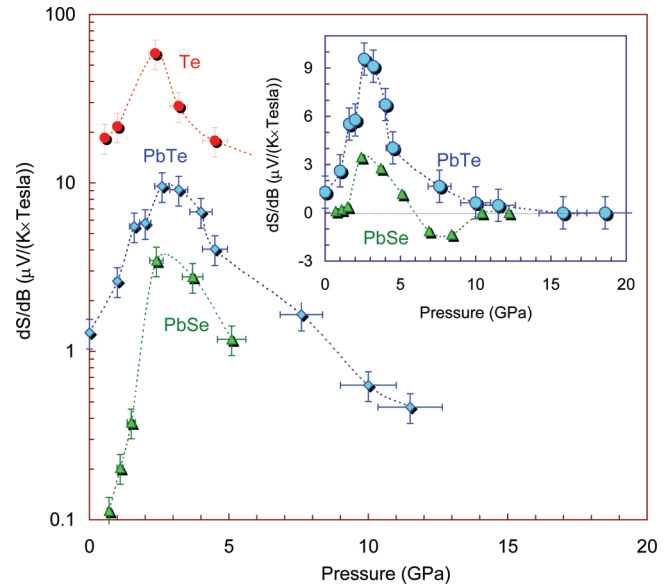


Figure 12. The pressure dependencies of magnetic field coefficients of the thermopower (dS/dB) in PbSe, PbTe, and Te determined by data of the transverse Nernst–Ettingshausen effect from refs 85, 186, 187. The inset shows the inversion of the coefficient in PbSe in the high-pressure phase above 5 GPa.⁸⁵

experimentally found effect in PbTe is a variation in the thermopower by $\sim 20 \mu\text{V/K}$ in a field of $\sim 1.9 \text{ T}$ at 2.6 GPa (Figure 11).⁸⁵ Hence, using the data from section 2.2, one can estimate ZT as follows: $ZT \approx T \times (S + \Delta S)^2 / (\rho \times \lambda) = 300 \text{ K} \times (220 - 270 \mu\text{V/K})^2 / (0.1 \text{ (m}\Omega \times \text{cm)}) \times 7.25 \text{ W/(K} \times \text{m)}) \sim 2$ and ~ 3 for $S = 200$ and $250 \mu\text{V/K}$, respectively. Notice that both a further increase in magnetic field (Figure 11) and an increase in the $\Delta x/\Delta y$ ratio (Figure 10c and eq 9) are expected to result in a more significant variation in the thermopower and hence in the higher TE performance.

Literature data on magnetic field effect on the thermopower in dependence on external applied pressure are reviewed for some semiconductors (PbTe, PbSe, Te) at Figure 12.^{85,104,186,187} The enhancement of the dS/dB coefficients (proportional to the coefficient of transverse N–E effect, Q from eq 8) with pressure in PbTe, PbSe, and Te (Figure 12) correlates with a narrowing of their direct energy gaps E_g that are related to mobility rising as follows: $\mu \sim 1/m \sim 1/E_g$.⁴ Elemental tellurium is known not to be a thermoelectric, while the existence of the giant magnetothermoelectric effects (up to $\sim 60 \mu\text{V}/(\text{K} \times \text{Tesla})$) (Figure 12)¹⁸⁷ hints that this semiconductor potentially could be good magnetothermoelectrics.

4. Comments on Practical Realization of High-Pressure Thermoelectric Elements and Devices

In the introduction we mentioned that a high pressure may be obtained not only in a variety of different chambers, but also in situ simulated by different means. For instance, it was demonstrated on examples of PbTe and PbSe films deposited on a substrate with a misfit lattice parameter (KCl, KBr, BaF_2 , etc.), that stresses inside the films can stabilize both the orthorhombic and CsCl-structured high-pressure phases,^{86,87} which usually appear above 4.5–6.5

and 13–16 GPa.^{149–154} A high-pressure treatment of materials can also trap and keep improved TE properties, e.g., Bi₂Te₃ and Bi_{0.5}Sb_{1.5}Te₃ crystals subjected to a torsion under pressure of 6 GPa demonstrated significantly enhanced TE parameters.^{189,190} If a sample is subjected to high pressure cycling across a series of reconstructive phase transitions, its mesostructure may be substantially changed, and hence, TE parameters may be also changed, for instance, owing to a worsening of thermal conductivity.⁷ Recently, it was demonstrated that temperature annealing under pressure for bulk ZnO can stabilize its high-pressure rock-salt-structured phase and keep it upon decompression to ambient pressure.¹⁹¹ Thus, there are different simulation possibilities for practical realization of high-pressure effects at ambient conditions, but in order to select an appropriate method, the mechanisms of high-pressure enhancement of the TE performance should be properly understood. At the moment, even in two systems considered (Bi₂Te₃, PbTe) the origins of the colossal improvement of their TE parameters under pressure are still not yet fully understood. Some of the high-pressure cells employed in experiments, for example the one shown in Figure 10a, may be used as prototypes for TE energy converters, in which a sample (or assembly of samples) serves as a working TE element.

5. Conclusion

The present review briefly summarizes the state-of-the-art achievements in high-pressure effects on the performance of energy conversion materials. The review focuses basically on two classical telluride systems, namely Bi₂Te₃ and PbTe, which a long time ago were proposed for thermoelectric applications and for this reason appear to be more studied than others. A detailed comparison of structural, optical, and transport properties suggests that these so-called conventional thermoelectrics under pressure became unconventional ultranarrow gap thermoelectrics. Therefore, pressure studies indicate that a current understanding of the thermoelectricity in these materials is not sufficient. The review also explains and gives examples how relatively weak magnetic fields can significantly improve the TE parameters. A possibility of multicascade improvement of the performance of TE elements is demonstrated on examples of combined effects of pressure and magnetic field. Applied pressure can change energy gap and charge carrier parameters. While the enhanced TE properties are usually achieved in a narrow-gap one-band semiconductor with several closely lying bands and high density of states in vicinity of chemical potential level, the significant magnetothermoelectric properties are expected in a direct-gap two-band semiconductor with low effective mass and high mobility of carriers. In summary, this review introduces high pressure as a powerful tool for improvement of the performance of thermoelectrics that opens new perspectives in this field.

Acknowledgment. We thank Prof. V.A. Kulbachinski (Physics Department, Moscow State University) for helpful

comments regarding Bi₂Te₃-based thermoelectrics. The authors thank four anonymous Referees for critical reading of the manuscript and useful comments.

References

- (1) Tritt, T. M. *Science* **1999**, *283*, 804.
- (2) Sales, B. C.; Mandrus, D.; Williams, R. K. *Science* **1996**, *272*, 1325.
- (3) DiSalvo, F. J. *Science* **1999**, *285*, 703.
- (4) Seeger, K. *Semiconductor Physics*; Springer-Verlag: Wien-N.Y, 1973.
- (5) Askerov, B. M. *Electronic Effects of Transfer in Semiconductors*; Nauka: Moscow, 1985.
- (6) Devyatkova, E. D.; Smirnov, I. A. *Soviet. Phys. Solid State* **1961**, *2*, 1786.
- (7) Sales, B. C. *Int. J. Appl. Ceram. Technol.* **2007**, *4*, 291.
- (8) Bhattacharya, S.; Pope, A. L.; Littleton, R. T.; Tritt, T. M.; Ponnambalam, V.; Xia, Y.; Poon, S. J. *Appl. Phys. Lett.* **2000**, *77*, 2476.
- (9) Wang, H.; Li, J. F.; Kita, T. *J. Phys. D: Appl. Phys.* **2007**, *40*, 6839.
- (10) Poudeu, P. F. P.; D'Angelo, J.; Kong, H.; Downey, A.; Short, J. L.; Pcionek, R.; Hogan, T. P.; Uher, C.; Kanatzidis, M. G. *J. Am. Chem. Soc.* **2006**, *128*, 14347.
- (11) Wang, H.; Li, J. F.; Nan, C. W.; Zhou, M.; Liu, W. S.; Zhang, B. P.; Kita, T. *Appl. Phys. Lett.* **2006**, *88*, 092104.
- (12) Jovovic, V.; Thiagarajan, S. J.; West, J.; Heremans, J. P.; Story, T.; Golacki, Z.; Paszkowicz, W.; Osinniy, V. *J. Appl. Phys.* **2007**, *102*, 043707.
- (13) Jovovic, V.; Thiagarajan, S. J.; Heremans, J. P.; Komissarova, T.; Khokhlov, D.; Nicorici, A. *J. Appl. Phys.* **2008**, *103*, 053710.
- (14) Yim, W. M.; Amith, A. *Solid-State Electron.* **1972**, *15*, 1141.
- (15) Hayashi, T.; Sekine, M.; Suzuki, J.; Horio, Y. *Mater. Trans.* **2006**, *47*, 1941.
- (16) Ahn, K.; Li, C.; Uher, C.; Kanatzidis, M. G. *Chem. Mater.* **2009**, *21*, 1361.
- (17) Lue, C. S.; Chou, M. D.; Kaurav, N.; Chung, Y. T.; Kuo, Y. K. *Appl. Phys. Lett.* **2009**, *94*, 192105.
- (18) Kutasov, V. A.; Luk'yanova, L. N.; Konstantinov, P. P. *Semiconductors* **2000**, *34*, 376.
- (19) Caylor, J. C.; Coonley, K.; Stuart, J.; Colpitts, T.; Venkatasubramanian, R. *Appl. Phys. Lett.* **2005**, *87*, 023105.
- (20) Sur, I.; Casian, A.; Balandin, A. *Phys. Rev. B* **2004**, *69*, 035306.
- (21) Beyer, H.; Nurnus, J.; Bottner, H.; Lambrecht, A.; Roch, T.; Bauer, G. *Appl. Phys. Lett.* **2002**, *80*, 1216.
- (22) Martin, J.; Nolas, G. S.; Zhang, W.; Chen, L. *Appl. Phys. Lett.* **2007**, *90*, 222112.
- (23) Ikeda, T.; Collins, L. A.; Ravi, V. A.; Gascoin, F. S.; Haile, S. M.; Snyder, G. J. *Chem. Mater.* **2007**, *19*, 763.
- (24) Sootsman, J. R.; Pcionek, R. J.; Kong, H.; Uher, C.; Kanatzidis, M. G. *Chem. Mater.* **2006**, *18*, 4993.
- (25) Koh, Y. K.; Vineis, C. J.; Calawa, S. D.; Walsh, M. P.; Cahill, D. G. *Appl. Phys. Lett.* **2009**, *94*, 153101.
- (26) Su, T. C.; Zhu, P. W.; Ma, H. A.; Ren, G. Z.; Chen, L. X.; Guo, W. L.; Iami, Y.; Jia, X. P. *Solid State Commun.* **2006**, *138*, 580.
- (27) Su, T.; Jia, X.; Ma, H.; Yu, F.; Tian, Y.; Zuo, G.; Zheng, Y.; Jiang, Y.; Dong, D.; Deng, L.; Qin, B.; Zhang, S. *J. Appl. Phys.* **2009**, *105*, 073713.
- (28) Tang, X. F.; Xie, W. J.; Li, H.; Zhang, W. Y.; Zhang, Q. J.; Niino, M. *Appl. Phys. Lett.* **2007**, *90*, 012102.
- (29) Cao, Y. Q.; Zhao, X. B.; Zhu, T. J.; Zhang, X. B.; Tu, J. P. *Appl. Phys. Lett.* **2008**, *92*, 143106.
- (30) Ma, Y.; Hao, Q.; Poudel, B.; Lan, Y.; Yu, B.; Wang, D.; Chen, G.; Ren, Z. F. *Nano Lett.* **2008**, *8*, 2580.
- (31) Poudel, B.; Hao, Q.; Ma, Y.; Lan, Y.; Minnich, A.; Yu, B.; Yan, X.; Wang, D.; Muto, A.; Vashae, D.; Chen, X.; Liu, J.; Dresselhaus, M. S.; Chen, G.; Ren, Z. F. *Science* **2008**, *320*, 634.
- (32) Venkatasubramanian, R.; Siivola, E.; Colpitts, T.; O'Quinn, B. *Nature* **2001**, *413*, 597.
- (33) Harman, T. C.; Taylor, P. J.; Walsh, M. P.; LaForge, B. E. *Science* **2002**, *297*, 2229.
- (34) Harman, T. C.; Walsh, M. P.; Laforge, B. E.; Turner, G. W. *J. Electron. Mater.* **2005**, *34*, L19.
- (35) Hsu, K. F.; Loo, S.; Guo, F.; Chen, W.; Dyck, J. S.; Uher, C.; Hogan, T.; Polychroniadis, E. K.; Kanatzidis, M. G. *Science* **2004**, *303*, 818.
- (36) Androulakis, J.; Hsu, K. F.; Pcionek, R.; Kong, H.; Uher, C.; D'Angelo, J. J.; Downey, A.; Hogan, T.; Kanatzidis, M. G. *Adv. Mater.* **2006**, *18*, 1170.
- (37) Zhou, M.; Li, J. F.; Kita, T. *J. Am. Chem. Soc.* **2008**, *130*, 4527.
- (38) Poudeu, P. F. P.; D'Angelo, J.; Downey, A. D.; Short, J. L.; Hogan, T. P.; Kanatzidis, M. G. *Angew. Chem., Int. Ed.* **2006**, *45*, 3835.
- (39) Heremans, J. P.; Jovovic, V.; Toberer, E. S.; Saramat, A.; Kurosaki, K.; Charoenphakdee, A.; Yamanaka, S.; Snyder, G. J. *Science* **2008**, *321*, 554.
- (40) Kurosaki, K.; Kosuga, A.; Muta, H.; Uno, M.; Yamanaka, S. *Appl. Phys. Lett.* **2005**, *87*, 061919.
- (41) Lowhorn, N. D.; Tritt, T. M.; Abbott, E. E.; Kolis, J. W. *Appl. Phys. Lett.* **2006**, *88*, 022101.

- (42) Littleton, R. T.; Tritt, T. M.; Feger, C. R.; Kolis, J.; Wilson, M. L.; Marone, M.; Payne, J.; Verebeli, D.; Levy, F. *Appl. Phys. Lett.* **1998**, *72*, 2056.
- (43) McGuire, M. A.; Reynolds, T. K.; DiSalvo, F. J. *Chem. Mater.* **2005**, *17*, 2875.
- (44) Matsumoto, H.; Kurosaki, K.; Muta, H.; Yamanaka, S. *J. Appl. Phys.* **2008**, *104*, 073705.
- (45) Terasaki, I.; Sasago, Y.; Uchinokura, K. *Phys. Rev. B* **1997**, *56*, 12685.
- (46) Chang, W. J.; Hsieh, C. C.; Chung, T. Y.; Hsu, S. Y.; Wu, K. H.; Uen, T. M.; Lin, J. -Y.; Lin, J. J.; Hsu, C. -H.; Kuo, Y. K.; Liu, H. L.; Hsu, M. H.; Gou, Y. S.; Juang, J. Y. *Appl. Phys. Lett.* **2007**, *90*, 061917.
- (47) Fujita, K.; Mochida, T.; Nakamura, K. *Jpn. J. Appl. Phys. part 1* **2001**, *40*, 4644.
- (48) Wang, Y. Y.; Rogado, N. S.; Cava, R. J.; Ong, N. P. *Nature* **2003**, *423*, 425.
- (49) Lee, M.; Viciu, L.; Li, L.; Wang, Y.; Foo, M. L.; Watauchi, S.; Pascal, R. A. jr; Cava, R. J.; Ong, N. P. *Nat. Mater.* **2003**, *5*, 537.
- (50) Nolas, G. S.; Cohn, J. L.; Slack, G. A.; Schujman, S. B. *Appl. Phys. Lett.* **1998**, *73*, 178.
- (51) Kuznetsov, V. L.; Kuznetsova, L. A.; Kaliazin, A. E.; Rowe, D. M. *J. Appl. Phys.* **2000**, *87*, 7871.
- (52) Sales, B. C.; Chakoumakos, B. C.; Jin, R.; Thompson, J. R.; Mandrus, D. *Phys. Rev. B* **2001**, *63*, 245113.
- (53) Blake, N. P.; Latturser, S.; Bryan, J. D.; Stucky, G. D.; Metiu, H. *J. Chem. Phys.* **2001**, *115*, 8060.
- (54) Cederkrantz, D.; Saramat, A.; Snyder, G. J.; Palmqvist, A. E. C. *J. Appl. Phys.* **2009**, *106*, 074509.
- (55) Aliev, F. G.; Brandt, N. B.; Moshchalkov, V. V.; Kozyrkov, V. V.; Skolozdra, R. V.; Belogorokhov, A. I. *Z. Phys. B: Condens. Matter* **1989**, *75*, 167.
- (56) Culp, S. R.; Simonson, J. W.; Poon, S. J.; Ponnambalam, V.; Edwards, J.; Tritt, T. M. *Appl. Phys. Lett.* **2008**, *93*, 022105.
- (57) Caillat, T.; Fleurial, J. P.; Borshchevsky, A. J. *Phys. Chem. Solids* **1997**, *58*, 1119.
- (58) Anh, D. T. K.; Tanaka, T.; Nakamoto, G.; Kurisu, M. *J. Alloys Compd.* **2006**, *421*, 232.
- (59) Brown, S. R.; Kaulzarich, S. M.; Gascoin, F.; Snyder, G. J. *Chem. Mater.* **2006**, *18*, 1873.
- (60) Ohta, S.; Nomura, T.; Ohta, H.; Hirano, M.; Hosono, H.; Koumoto, K. *Appl. Phys. Lett.* **2005**, *87*, 092108.
- (61) Ohta, H.; Kim, S.; Mune, Y.; Mizoguchi, T.; Nomura, K.; Ohta, S.; Nomura, T.; Nakanishi, Y.; Ikuhara, Y.; Hirano, M.; Hosono, H.; Koumoto, K. *Nat. Mater.* **2007**, *6*, 129.
- (62) Hochbaum, A. I.; Chen, R.; Delgado, R. D.; Liang, W.; Garnett, E. C.; Najarian, M.; Majumdar, A.; Yang, P. *Nature* **2008**, *451*, 163.
- (63) Boukai, A. I.; Bunimovich, Y.; Tahir-Kheli, J.; Yu, J.-K.; Goddard, W. A., III; Heath, J. R. *Nature* **2008**, *451*, 168.
- (64) Ioffe, A. F. *Semiconductor Thermoelements and Thermoelectric Cooling*; InfoSerach: London, 1957.
- (65) Sofo, G. O.; Mahan, G. D. *Phys. Rev. B* **1994**, *49*, 4565.
- (66) Chasmar, R.; Stratton, R. J. *Electron. Control* **1959**, *7*, 52.
- (67) Mahan, G. D. *J. Appl. Phys.* **1989**, *65*, 1578.
- (68) Yamaguchi, S.; Iwamura, Y.; Yamamoto, A. *Appl. Phys. Lett.* **2003**, *82*, 2065.
- (69) Yamaguchi, S.; Izaki, R.; Kaiwa, N.; Sugimura, S.; Yamamoto, A. *Appl. Phys. Lett.* **2004**, *84*, 5344.
- (70) Izaki, R.; Kaiwa, N.; Hoshino, M.; Yaginuma, T.; Yamaguchi, S.; Yamamoto, A. *Appl. Phys. Lett.* **2005**, *87*, 243508.
- (71) Izaki, R.; Hoshino, M.; Yaginuma, T.; Kaiwa, N.; Yamaguchi, S.; Yamamoto, A. *Microelectron. J.* **2007**, *38*, 667.
- (72) Butcher, K. S. A.; Tansley, T. L. *Superlattices Microstruct.* **2005**, *38*, 1.
- (73) Pantha, B. N.; Dahal, R.; Li, J.; Lin, J. Y.; Jiang, H. X.; Pomrenke, G. *Appl. Phys. Lett.* **2008**, *92*, 042112.
- (74) Shi, X. Y.; Huang, F. Q.; Liu, M. L.; Chen, L. D. *Appl. Phys. Lett.* **2009**, *94*, 122103.
- (75) Sevik, C.; Çağın, T. *Appl. Phys. Lett.* **2009**, *95*, 112105.
- (76) Steglich, F.; Aarts, J.; Bredl, C. D.; Lieke, W.; Meschede, D.; Franz, W.; Schafer, H. *Phys. Rev. Lett.* **1979**, *43*, 1892.
- (77) Yuan, H. Q.; Grosche, F. M.; Deppe, M.; Geibel, C.; Sparn, G.; Steglich, F. *Science* **2003**, *302*, 2104.
- (78) Aust, R. B.; Samara, G. A.; Drickamer, H. *J. Chem. Phys.* **1964**, *41*, 2003.
- (79) Shirovani, I.; Onodera, A.; Anzai, H. *J. Solid State Chem.* **1981**, *36*, 246.
- (80) Kagoshima, S.; Kondo, R.; Matsushita, N.; Higa, M.; Ovsyannikov, S. V.; Shaydarova, N. A.; Shchennikov, V. V.; Manakov, A. Y.; Likhacheva, A. Y. *Phys. Status Solidi B* **2007**, *244*, 418.
- (81) Zhang, F.; Crespi, V. H.; Zhang, P. *Phys. Rev. Lett.* **2009**, *102*, 156401.
- (82) Shimizu, K.; Suhara, K.; Ikumo, M.; Eremets, M. I.; Amaya, K. *Nature* **1998**, *393*, 767.
- (83) Ma, Y.; Eremets, M.; Oganov, A. R.; Xie, Y.; Trojan, I.; Medvedev, S.; Lyakhov, A. O.; Valle, M.; Prakapenka, V. *Nature* **2009**, *458*, 182.
- (84) Ovsyannikov, S. V.; Shchennikov, V. V.; Vorontsov, G. V.; Manakov, A. Y.; Likhacheva, A. Y.; Kulbachinskii, V. A. *J. Appl. Phys.* **2008**, *104*, 053713.
- (85) Shchennikov, V. V.; Ovsyannikov, S. V. *Solid State Commun.* **2003**, *126*, 373.
- (86) Baleva, M.; Mateeva, E. *Phys. Rev. B* **1994**, *50*, 8893.
- (87) Baleva, M.; Momtchilova, M. *Phys. Rev. B* **1994**, *50*, 15056.
- (88) Zhu, P. W.; Jia, X.; Chen, H. Y.; Chen, L. X.; Guo, W. L.; Mei, D. L.; Liu, B. B.; Ma, H. A.; Ren, G. Z.; Zou, G. T. *Chem. Phys. Lett.* **2002**, *359*, 89.
- (89) Gerlich, D. *J. Phys. C: Solid State Phys.* **1982**, *15*, 3305.
- (90) Hofmeister, A. M. *Science* **1999**, *283*, 1699.
- (91) Hofmeister, A. M. *Proc. Nat. Acad. Sci.* **2007**, *104*, 9192.
- (92) Saxena, S. K.; Shen, G.; Lazor, P. *Science* **1994**, *264*, 405.
- (93) Goncharov, A. F.; Beck, P.; Struzhkin, V. V.; Haugen, B. D.; Jacobsen, S. D. *Phys. Earth Planet. Int.* **2009**, *174*, 24–32.
- (94) Ross, R. G.; Andersson, P.; Sundqvist, B.; Backstrom, G. *Rep. Prog. Phys.* **1984**, *47*, 1347.
- (95) Hakansson, B.; Andersson, P.; Backstrom, G. *Rev. Sci. Instrum.* **1988**, *59*, 2269.
- (96) Talyzin, A. V.; Andersson, O.; Sundqvist, B.; Kurnosov, A.; Dubrovinsky, L. *J. Solid State Chem.* **2007**, *180*, 510.
- (97) Heremans, J. P.; Thrush, C. M.; Morelli, D. T. *Phys. Rev. Lett.* **2001**, *86*, 2098.
- (98) Ertl, M. E.; Pfister, G. R.; Goldsmid, H. J. *British J. Appl. Phys.* **1963**, *14*, 161.
- (99) Boikov, Y. A.; Goltsman, B. M.; Danilov, V. A. *Semiconductors* **1995**, *29*, 464.
- (100) Zemskov, V. S.; Belaya, A. D.; Beluy, U. S.; Kozhemyakin, G. N. *J. Cryst. Growth* **2000**, *212*, 161.
- (101) Sun, Y.; Salamon, M. B.; Lee, M.; Rosenbaum, T. F. *Appl. Phys. Lett.* **2003**, *82*, 1440.
- (102) Hasegawa, Y.; Ishikawa, Y.; Komine, T.; Huber, T. E.; Suzuki, A.; Morita, H.; Shirai, H. *Appl. Phys. Lett.* **2004**, *85*, 915.
- (103) Teramoto, T.; Komine, T.; Yamamoto, S.; Kuraishi, M.; Sugita, R.; Hasegawa, Y.; Nakamura, H. *J. Appl. Phys.* **2008**, *104*, 053714.
- (104) Shchennikov, V. V.; Ovsyannikov, S. V.; Bazhenov, A. V. *J. Phys. Chem. Solids* **2008**, *69*, 2315.
- (105) Wright, D. A. *Nature* **1958**, *181*, 834.
- (106) Goldsmid, H. J. *J. Appl. Phys.* **1961**, *32*, 2198.
- (107) Atabaeva, E. Y.; Bendeliani, N. A.; Popova, S. P. *Fiz. Tverdogo Tela* **1973**, *15*, 3508.
- (108) Iina, M. A.; Itskevich, E. S. *Soviet Phys.-Solid State, USSR* **1972**, *13*, 2098.
- (109) Vereshchagin, L. F.; Bendeliani, N. A.; Atabaeva, E. Y. *Soviet Phys.-Solid State, USSR* **1972**, *13*, 2051.
- (110) Iina, M. A.; Itskevich, E. S. *Fiz. Tverdogo Tela* **1975**, *17*, 154.
- (111) Khvostantsev, L. G.; Orlov, A. I.; Abrikosov, N. K.; Svecnikova, T. E.; Chizhevskaya, S. N. *Phys. Status Solidi A* **1982**, *71*, 49.
- (112) Polvani, D. A.; Meng, J. F.; Chandra Shekar, N. V.; Sharp, J.; Badding, J. V. *Chem. Mater.* **2001**, *13*, 2068.
- (113) Jacobsen, M. K.; Kumar, R. S.; Cornelius, A. L.; Sinogeiken, S. V.; Nicol, M. F. *AIP Conf. Proc.* **2007**, *955*, 171.
- (114) Nakayama, A.; Einaga, M.; Tanabe, Y.; Nakano, S.; Ishikawa, F.; Yamada, Y. *High Pressure Res.* **2009**, *29*, 245.
- (115) Kulbachinskii, V. A.; Shennikov, V. V.; Gorac, J.; Locziak, P. *Fiz. Tverdogo Tela* **1994**, *36*, 526.
- (116) Li, C. Y.; Ruoff, A. L.; Spencer, C. W. *J. Appl. Phys.* **1961**, *32*, 1733.
- (117) Goltsman, B. M.; Kudinov, B. A.; Smirnov, I. A. *Thermoelectric Semiconductor Materials Based on Bi₂Te₃*; Nauka: Moscow, 1972.
- (118) Sologub, V. V.; Parfenev, R. V.; Goletskaya, A. D. *JETP Lett* **1975**, *21*, 337.
- (119) Mishra, S. K.; Satpathy, S.; Jepsen, O. *J. Phys.: Condens. Matter* **1997**, *9*, 461.
- (120) Greanya, V. A.; Tonjes, W. C.; Liu, R.; Olson, C. G.; Chung, D. -Y.; Kanatzidis, M. G. *Phys. Rev. B* **2000**, *62*, 16425.
- (121) Yoon, S. J.; Freeman, A. J. *Phys. Rev. B* **2001**, *63*, 085112.
- (122) Larson, P.; Greanya, V. A.; Tonjes, W. C.; Liu, R.; Mahanti, S. D.; Olson, C. G. *Phys. Rev. B* **2002**, *65*, 085108.
- (123) Wang, G.; Cagin, T. *Phys. Rev. B* **2007**, *76*, 075201.
- (124) Thonhauser, T.; Scheidemantel, T. J.; Sofo, J. O.; Badding, J. V.; Mahan, G. D. *Phys. Rev. B* **2003**, *68*, 085201.
- (125) Zhang, H.; Liu, C. -X.; Qi, X. -L.; Dai, X.; Fang, Z.; Zhang, S. -C. *Nature Phys.* **2009**, *5*, 438.
- (126) Chen, Y. L.; Analytis, J. G.; Chu, J. -H.; Liu, Z. K.; Mo, S. -K.; Qi, X. L.; Zhang, H. J.; Lu, D. H.; Dai, X.; Fang, Z.; Zhang, S. C.; Fisher, I. R.; Hussain, Z.; Shen, Z. -X. *Science* **2009**, *325*, 178.
- (127) Yamashita, O.; Tomiyoshi, S.; Makita, K. *J. Appl. Phys.* **2003**, *93*, 368.
- (128) Meng, J. F.; Shekar, N. V. C.; Badding, J. V.; Chung, D. Y.; Kanatzidis, M. G. *J. Appl. Phys.* **2001**, *90*, 2836.
- (129) Nishigori, S.; Araki, H.; Kitagawa, H.; Hasezaki, K. Thermoelectric Measurements on Bi_{0.5}Sb_{1.5}Te₃ under Hydrostatic Pressure. In *Proceedings of XXV International Conference on Thermoelectrics*; Vienna, Austria, Aug. 6–10, 2006; p 556–557.
- (130) Khvostantsev, L. G.; Orlov, A. I.; Abrikosov, N. K.; Ivanova, L. D. *Phys. Status Solidi A* **1980**, *58*, 37.
- (131) Itskevich, E. S.; Popova, S. P.; Atabaeva, E. Y. *Dokl. Akad. Nauk USSR* **1963**, *153*, 306.
- (132) Manga, M.; Jeanloz, R. J. *Geophys. Res.* **1997**, *102B*, 2999.
- (133) Averkin, A. A.; Zhaparov, Z. Z.; Stilbans, L. S. *Soviet Phys. Semicond.-USSR* **1972**, *5*, 1954.
- (134) Larson, P. *Phys. Rev. B* **2006**, *74*, 205113.

- (135) Chandra Shekar, N. V.; Polvani, D. A.; Meng, J. F.; Badding, J. V. *Phys. B* **2005**, *358*, 14, and references therein.
- (136) Itskevich, E. S.; Kashirskaya, L. M.; Kraidenov, V. F. *Semiconductors* **1997**, *31*, 276.
- (137) Kulbachinskii, V. A.; Klokoval, N. E.; Gorak, J.; Lostjak, P.; Azou, S. A.; Mironova, G. A. *Fiz. Tverdogo Tela* **1989**, *31*, 205.
- (138) Kullmann, W.; Geurts, J.; Richter, W.; Lehner, N.; Rauh, H.; Steigenberger, U.; Eichhorn, G.; Geick, R. *Phys. Status Solidi B* **1984**, *125*, 131.
- (139) Peranio, N.; Eibl, O. *J. Appl. Phys.* **2008**, *103*, 024314.
- (140) Meng, J. F.; Shekar, N. V. C.; Chung, D.-Y.; Kanatzidis, M.; Badding, J. V. *J. Appl. Phys.* **2003**, *94*, 4485.
- (141) Liufu, S. C.; Chen, L. D.; Yao, Q.; Wang, C. F. *Appl. Phys. Lett.* **2007**, *90*, 112106.
- (142) Chen, F.; Fang, J.; Stokes, K. L.; Stern, A.; MacLaren, J. Thermopower of Bi₂S₃ Under High Pressure. In APS Meeting, March, **2002**; Abs. S660008.
- (143) Dughhaish, Z. H. *Phys. B* **2002**, *322*, 205.
- (144) *Numerical Data and Functional Relationships in Science and Technology Landolt-Bornstein*, New Series; Madelung, O., Schulz, M., Weiss, H., Eds.; Springer: Berlin, 1983; Vol. 17.
- (145) Ravich, Y. I.; Efimova, B. A.; Smirnov, I. A. *Semiconducting Lead Chalcogenides*; Nauka: Moscow, 1968; Plenum: New York, 1970.
- (146) Besson, J. M.; Paul, W.; Calawa, A. R. *Phys. Rev.* **1968**, *173*, 699.
- (147) Schluter, M.; Martinez, G.; Cohen, M. L. *Phys. Rev. B* **1975**, *12*, 650.
- (148) Brandt, N. B.; Gitsu, D. V.; Popovich, N. S.; Sidorov, V. I.; Chudinov, S. M. *JETP Lett.* **1975**, *22*, 104.
- (149) Fujii, Y.; Kitamura, K.; Onodera, A.; Yamada, Y. *Solid State Commun.* **1984**, *49*, 135.
- (150) Chattopadhyay, T.; Von Schnering, H. G.; Grosshans, W. A.; Halzapfel, W. B. *Phys. BC* **1986**, *139-140*, 356.
- (151) Rouse, G.; Klotz, S.; Saitta, A. M.; Rodriguez-Carvajal, J.; McMahon, M. I.; Couzinet, B.; Mezouar, M. *Phys. Rev. B* **2005**, *71*, 224116.
- (152) Shchennikov, V. V.; Ovsyannikov, S. V.; Manakov, A. Y.; Likhacheva, A. Y.; Ancharov, A. I.; Berger, I. F.; Sheromov, M. A. *JETP Lett.* **2006**, *83*, 228.
- (153) Ovsyannikov, S. V.; Shchennikov, V. V.; Manakov, A. Y.; Likhacheva, A. Y.; Ponosov, Y. S.; Mogilenskikh, V. E.; Vokhmyanin, A. P.; Ancharov, A. I.; Skipetrov, E. P. *Phys. Status Solidi B* **2009**, *246*, 615.
- (154) Shchennikov, V. V.; Ovsyannikov, S. V.; Derevskov, A. Y. *Phys. Solid State* **2002**, *44*, 1845.
- (155) Wang, Y.; Chen, X.; Cui, T.; Niu, Y.; Wang, Y.; Wang, M.; Ma, Y.; Zou, G. *Phys. Rev. B* **2007**, *76*, 155127.
- (156) Streltsov, S. V.; Manakov, A. Y.; Vokhmyanin, A. P.; Ovsyannikov, S. V.; Shchennikov, V. V. *J. Phys.: Condens. Matter* **2009**, *21*, 385501.
- (157) Averkin, A. A.; Moizhes, B. Y.; Smirnov, I. A. *Soviet Phys.-Solid State* **1961**, *3*, 1354.
- (158) Averkin, A. A.; Dombrovskaya, I. G.; Moizhes, B. Y. *Soviet Phys.-Solid State* **1963**, *5*, 66.
- (159) Ovsyannikov, S. V.; Shchennikov, V. V.; Popova, S. V.; Derevskov, A. Y. *Phys. Status Solidi B* **2003**, *235*, 521.
- (160) Ovsyannikov, S. V.; Shchennikov, V. V. *Phys. Status Solidi B* **2004**, *241*, 3231.
- (161) Ovsyannikov, S. V.; Shchennikov, V. V. *Appl. Phys. Lett.* **2007**, *90*, 122103.
- (162) Ren, G.-Z.; Jia, X.-P.; Zhu, P.-W.; Zang, C.-Y.; Ma, H.-A.; Wang, X.-C. *Chin. Phys. Lett.* **2005**, *22*, 236.
- (163) McGuire, M. A.; Malik, A. S.; DiSalvo, F. J. *J. Alloys Compd.* **2008**, *460*, 8.
- (164) Lu, W.; Fang, J.; Stokes, K. L.; Lin, J. *J. Am. Chem. Soc.* **2004**, *126*, 11798.
- (165) Wang, W.; Poudel, B.; Wang, D.; Ren, Z. F. *Adv. Mater.* **2005**, *17*, 2110.
- (166) Zhu, J. P.; Yu, S. H.; He, Z. B.; Jiang, J.; Chen, K.; Zhou, X. Y. *Chem. Commun.* **2005**, 5802.
- (167) Tong, H.; Zhu, Y. J.; Yang, L. X.; Li, L.; Zhang, L. *Angew. Chem., Int. Ed.* **2006**, *45*, 7739.
- (168) Zhang, G.; Lu, X.; Wang, W.; Li, X. *Chem. Mater.* **2007**, *19*, 5207.
- (169) Li, G. R.; Yao, C. Z.; Lu, X. H.; Zheng, F. L.; Feng, Z. P.; Yu, X. L.; Su, C. Y.; Tong, Y. X. *Chem. Mater.* **2008**, *20*, 3306.
- (170) Skipetrov, E. P.; Zvereva, E. A.; Volkova, O. S.; Golubev, A. V.; Mollaev, A. Y.; Arslanov, R. K.; Slyn'ko, V. E. *Semiconductors* **2004**, *38*, 1164.
- (171) Gelbstein, Y.; Dashevsky, Z.; Dariel, M. P. *J. Appl. Phys.* **2008**, *104*, 033702.
- (172) Meng, J. F.; Polvani, D. A.; Janes, C. D. W.; DiSalvo, F. J.; Fei, Y.; Badding, J. V. *Chem. Mater.* **2000**, *12*, 197.
- (173) Chen, F.; Stokes, K. L.; Funahashi, R. *Appl. Phys. Lett.* **2002**, *81*, 2379.
- (174) Chen, F.; Stokes, K. L.; Nolas, G. S. *J. Phys. Chem. Solids* **2002**, *63*, 827.
- (175) Tsidilkovskii, I. M.; Shchennikov, V. V.; Gluzman, N. G. *Soviet Phys. Semicond.-USSR* **1983**, *17*, 604.
- (176) Chen, X.; Wang, Y.; Cui, T.; Ma, Y.; Zou, G.; Iitaka, T. *J. Chem. Phys.* **2008**, *128*, 194713.
- (177) Tsiok, O. B.; Khvostantsev, L. G.; Smirnov, I. A.; Golubkov, A. V. *J. Exp. Theor. Phys.* **2005**, *100*, 752.
- (178) Agarwal, A.; Trivedi, P. H.; Lakshminarayana, D. *Cryst. Res. Technol.* **2005**, *40*, 789.
- (179) Tsidilkovskii, I. M. *Thermomagnetic Effects in Semiconductors*; Infosearch Ltd: London, 1962.
- (180) Shchennikov, V. V.; Ovsyannikov, S. V. *JETP Lett.* **2003**, *77*, 88.
- (181) Chernenik, I. A.; Kaidanov, V. I.; Vinogradova, M. I.; Kolomoets, N. V. *Soviet Phys. Semicond.* **1968**, *2*, 645.
- (182) Heremans, J. P.; Thrush, C. M.; Morelli, D. T. *Phys. Rev. B* **2004**, *70*, 115334.
- (183) Aksel'rod, M. M.; Demchuk, K. M.; Tsidil'kovskii, I. M. *Phys. Status Solidi* **1968**, *27*, 249.
- (184) Averkin, A. A.; Gryznov, O. S.; Sanfirov, Y. Z. *Soviet Phys. Semicond.-USSR* **1976**, *10*, 350.
- (185) Averkin, A. A.; Gryznov, O. S.; Sanfirov, Y. Z. *Soviet Phys. Semicond.-USSR* **1978**, *12*, 1358.
- (186) Shchennikov, V. V.; Ovsyannikov, S. V. *JETP Letters* **2001**, *74*, 486.
- (187) Ovsyannikov, S. V.; Shchennikov, V. V. *Phys. B* **2004**, *344*, 190.
- (188) Ansel'm, A. I. *Introduction to Semiconductor Theory*; Nauka: Moscow, 1978.
- (189) Ashida, M.; Hamachiyo, T.; Hasezaki, K.; Matsunoshita, H.; Kai, M.; Horita, Z. *J. Phys. Chem. Solids* **2009**, *70*, 1089.
- (190) Hamachiyo, T.; Ashida, M.; Hasezaki, K.; Matsunoshita, H.; Kai, M.; Horita, Z. *Mater. Transactions* **2009**, *50*, 1592.
- (191) Bayarjargal, L.; Winkler, B.; Haussühl, E.; Boehler, R. *Appl. Phys. Lett.* **2009**, *95*, 061907.
- (192) Shchennikov, V. V.; Stepanov, N. N.; Smirnov, I. A.; Golubkov, A. V. *Fiz. Tverdogo Tela* **1988**, *30*, 3105.